

Pulse propagation in a resonant medium: Application to sound waves in superfluid $^3\text{He-B}$

E. Varoquaux

Laboratoire de Physique des Solides, Université de Paris—Sud, F-91405 Orsay, France

G. A. Williams

Department of Physics, University of California, Los Angeles, California 90024

O. Avenel

*Service de Physique du Solide et de Résonance Magnétique, Centre d'Etudes Nucléaires de Saclay,
F-91191 Gif-sur-Yvette Cedex, France*

(Received 28 March 1986)

We give a description of the propagation of pulsed signals in a resonant medium based both on a time-domain analytical solution of the problem and on experimental observations in superfluid ^3He . These signals propagate according to a wave equation involving the unperturbed velocity c_0 and coupled to an internal mode characterized by a resonance frequency ω_m , an oscillator strength λ , and a lifetime τ . This mode crossing situation may exhibit a region of anomalous dispersion for which $d\omega/dk < 0$; this leads to well-known difficulties in the application of the concept of group velocity to wave packets with center frequency in the neighborhood of ω_m . We tackle this problem as follows. Using the slowly varying envelope approximation, we transform the Fourier integral representing the general wave propagation solution at location x and retarded local time $t' = t - x/c_0$ into a time-convolution integral for the wave envelope. We then split this time integral into a short-local-time part and a long-time part. Depending on circumstances, the short-time part is either the signal itself (far from ω_m or if it varies rapidly with respect to τ) or a precursory motion which is akin to Sommerfeld's precursor and which has already been discussed from another point of view by Crisp and others. The envelope of these precursors behaves as $(t'/\Lambda x)^n J_n(2\sqrt{\Lambda x t'})$, with $\Lambda = \lambda\omega_0^2/2c_0$, n being the order of the first nonzero derivative of the envelope at the origin ($x=0$). As the flight path in the resonant medium increases, it decays as a power of $x^{-1/2}$ only and its pseudofrequency $\Lambda x/2\pi$ increases. This part of the response, which we call a resonant precursor of order n , arises from the free response of the Lorentz oscillators to their own field and decays in time as $\exp(-t'/\tau)$. Characteristic wiggling patterns of this kind have been observed in sound propagation measurements in superfluid ^3He , described below in detail, and, more recently on an optical system using ultrashort laser pulses by Rothenberg, Grischkowsky, and Balant. The long-time part of the convolution integral describes the gradual distortion of the envelope as it propagates. This leads to the concept of complex group velocity, already introduced by Johnson, and shows its general applicability: pulses smooth on time scale τ propagate with the classical group velocity as long as causality is preserved. This result, already stated for Gaussian pulses by Garrett and McCumber, is compared critically to the early and conflicting predictions on signal propagation velocity made by Brillouin and by Baerwald. Thus, for signals which are not very short, the received envelope is made up of two parts, precursors, which travel with velocity c_0 , and a delayed signal which is damped exponentially, and travels with the classical group velocity and, close to resonance, suffers distortion governed by the size of dA/dt with respect to A . Computer simulations illustrate these different concepts.

I. INTRODUCTION

The problem of wave propagation of an acoustic or electromagnetic field in a medium which interacts with this field is as old as the theory of partial-differential equations. This quite general and fundamental problem is still arousing interest in linear¹ as well as nonlinear situations² because a number of questions are left without fully satisfactory answers. In this paper we consider the propagation of wave packets, or pulsed signals, in a resonant medium where the wave of finite duration interacts with a well-defined mode internal to the matter sustaining the

wave. Such a situation of mode crossing occurs in various fields of physics, optics, plasma physics, acoustics, etc., where the same concepts of group or signal velocities and precursory motion are met. These concepts are defined and used in a number of textbooks, e.g., Refs. 1–5. However, as will become apparent below, basic questions such as the arrival time of the wave packet at a specified location x , or the applicability of the concept of group velocity, or even the very significance of the notions of signal and transients, are not yet given clearcut and universally acknowledged answers. Our aim here is to study the case of weakly coupled modes with finite lifetime in a perfectly

homogeneous medium. Our approach is in part experimental and we have already reported conclusive observations of precursors and precise measurement of signal velocities.⁶ We also tackle the problem from an analytical point of view which, by a fairly straightforward time-domain analysis, leads to simple expressions for the signal velocity and the properties of precursors. Some of these analytical results, the consequences of which have been checked and extended by computer simulations, have been presented in a short communication.⁷

These topics of general interest have been extensively covered in the literature by a large number of authors and surveyed from a general point of view in 1948 by Eckart⁸ and in 1976 by Wainshtein.⁹ An extensive review of the early studies of light propagation in matter has been made by Brillouin in his well-known book on wave propagation and group velocity.¹ Basic questions on the causality of the medium response, the splitting of that response between free and forced oscillations giving rise to a forerunning part propagating with the velocity of light in vacuum, c , and a bulk part propagating with the group velocity received satisfactory answers at about the time at which the theory of special relativity gained full recognition.^{5,10} The mathematical tool of asymptotic evaluation of Fourier integrals, introduced in the problem by Brillouin,¹¹ led him to a thorough discussion of the various velocities involved in the propagation of a wave packet. As is well known, these velocities are (1) the phase velocity of the wave $c_p = \omega/k$ linked to the propagation of a plane wave $\exp[-i(\omega t - kx)]$, (2) the group velocity $c_g = d\omega/dk$ of propagation of a disturbance of the plane wave, (3) the energy velocity c_e related to the flux of energy given by Poynting's vector, and (4) the signal velocity c_s governing the propagation of a wave front understood as a signal transmitted from one observer to another and carrying some information such as a synchronizing beat between two clocks. The last three velocities do not differ much from one another, except when the wave vector k is varying rapidly with frequency. This happens, for instance, close to the center frequency of a resonance absorption line where $d\omega/dk$, that is, c_g , may become larger than c , infinite, or even negative. In such a case where the dispersion is said to be anomalous, the concept of group velocity was widely considered physically irrelevant. In place of that quantity, Brillouin introduced the signal velocity, defined operationally by the arrival time of the signal. Such a velocity is bound to possess a meaning in all situations in which a wave propagates, including the anomalous dispersion region where pulse shapes are severely distorted. But it turned out that this concept was also subject to difficulties because a refinement of Brillouin's work by Baerwald¹² led to a quite different behavior for c_s . Brillouin's prediction is that, close to ω_m , c_s is nearly equal to c_p , and hence c , without ever exceeding this maximum limit. Baerwald's findings, which are supported by a number of more recent studies,¹³⁻¹⁷ yield a monotonous retardation of the signal in the anomalous dispersion region: The signal velocity reaches a minimum at the center of the resonance line. According to Brillouin's own words,¹ any value for c_s between these widely different predictions can be found, de-

pending on the sensitivity of the detector used. We shall show below how this statement can be qualified and reformulated in a more satisfactory manner.

The first experimental study of signal velocity in a region of resonant absorption was performed in 1962 by Shiren^{18,19} using ultrasonic techniques. Absorption and arrival-time measurements were made on pulsed ultrasonic waves propagating in single-crystal MgO and interacting with paramagnetic-resonance absorption lines of Ni^{2+} and Fe^{2+} impurity ions. Owing to the presence of large-scale inhomogeneities in the sample, these experiments did not provide clues stringent enough to differentiate between Brillouin's and Baerwald's predictions.

A few years later, Garrett and McCumber²⁰ discovered, using analytical expressions and computer experiments, that light pulses of Gaussian shape, as will be discussed below, propagate seemingly undistorted with velocities close to the classical group velocity even in regions where c_g is faster than light in vacuum or even negative. This prediction, confirmed by Crisp²¹ and others,²² and discussed more recently by Macke²³ and in Ref. 7, is paradoxical in appearance only and quickly led to experimental observations of superluminal velocities.²⁴ More recently, the existence of negative velocities following the classical group-velocity formula throughout the anomalous region has been established experimentally by Chu and Wong²⁵ using laser pulses coupled to an excitonic line of GaP:N. Even more precise experiments with a true shape detection of the Gaussian pulse have been reported very recently by Segard and Macke²⁶ in the microwave domain.

As we shall show, this behavior is not limited to Gaussian pulses, but can be extended to a much wider class of pulse shapes. The first example, to our knowledge, of signal propagation as discussed by Brillouin of non-bell-shaped pulses can be seen in Ref. 27. These observations have led to the more detailed study of Ref. 6, which is described in full below and which clearly shows a reacceleration of the signal in the anomalous dispersion region. However, this work also reveals the importance of the somewhat mysterious phenomenon of precursors. This phenomenon is another major contribution of Sommerfeld and Brillouin,^{1,10,11} who realized²⁸ that some frequency components of a wide spectrum pulse had to propagate at or very close to light-in-vacuum velocities. These components are attenuated less than the signal components whose frequencies lie closer to the absorption band and add up to a significant contribution after a sizable flight path in the medium. These ideas were taken up by Baerwald¹² and a number of authors^{14,15,29,30} afterward. This wide acceptance, together with the very name of precursors (adopted from the field of seismology,³¹ where precursory waves are quite commonly observed) suggests that the effect is well studied and its properties well known. This is not the case, as the first direct experimental search for precursors was only reported in 1969 by Pleshko and Palócz³² on a waveguide with a controllable stop band. In this well-defined artificial medium, the high-frequency Sommerfeld precursor and low-frequency Brillouin precursor were clearly identified.

In the late 1960's interest in the propagation of strong

short pulses was renewed because of the discovery by McCall and Hahn^{33,34} of coherent effects between light and matter, giving rise to a self-induced transparency of the medium. The occurrence of transparency is governed by the area theorem, which states that when the time integral of the pulse amplitude expressed in suitable reduced units is equal to $2n\pi$, the pulse evolves towards a stable shape which propagates unattenuated and undistorted as a result of the coherent and nonlinear interaction with the absorbing medium. The $n=0$ case of the theorem, i.e., the 0π pulse, is in a sense degenerate. It may refer either to a strongly nonlinear case, as a combination of “ $+2\pi$ ” and “ -2π ” pulses (or “breather”), or else to the linear limit of small short pulses. The latter situation was studied by Crisp^{35,36} and others.³⁷ Under circumstances which will be described in detail below, such short pulses of small amplitude exhibit pulse breakup and develop characteristic Bessel-function oscillations. Pulse reshaping and the transparency arising from the 0π structure, in accordance with the area theorem, have been observed in a number of experiments.³⁸⁻⁴⁴ A direct recognition of the shape of the 0π structure was performed by acoustic techniques on the near-ideally-homogeneous and coherent case of superfluid $^3\text{He-B}$ in Ref. 6. Our work was followed not long after by the picosecond shape detection of short laser pulses propagating through a dilute Lorentz gas by Rothenberg *et al.*⁴⁵ The outcomes of the acoustic and optical experiments are remarkably similar and a detailed analysis maps them very precisely into Crisp's 0π pattern. This pattern is generated by rapidly varying portions of the wave packet and travels with the fastest velocity compatible with causal response. There is no question that it constitutes a precursor in spite of the fact that this possibility was ruled out by Crisp.³⁵ We shall show how to reconcile this last author's point of view with our presentation. We shall also put forward the idea that the 0π structure has the same physical origin and the same analytical form (within variants to be specified) as Sommerfeld's precursor and should be considered another facet of the same phenomenon.⁴⁶

Our contribution to these problems, as already mentioned, has been spurred by experiments on sound-wave propagation in superfluid $^3\text{He-B}$. In order to analyze our results, we have developed an analytical approach to the resonant-propagation problem in an idealized Lorentzian medium. The conditions under which the Lorentzian case applies are dealt with below, in Sec. II. In Sec. III we further restrict the problem to pulses whose frequency spectrum does not extend over a range very much larger than the anomalous dispersion region, but does cover it, in contrast with the conventional frequency-domain approach.^{1,3,5} In this region the medium dispersion law is approximated by the following expression:

$$k(\omega) = \frac{\omega}{c} - \frac{\Lambda}{\omega - \omega_m + i/\tau} \quad (1)$$

The Lorentz oscillators in the medium are characterized by their oscillator strength Λ and a relaxation time τ . The wave packet received at x is expressed as a Fourier integral involving the spectrum $\rho(\omega)$ of the initial pulse at the emitter ($x=0$),

$$\rho(t, x) = \int_{-\infty}^{+\infty} \rho(\omega) \exp[-i(\omega t - kx)] d\omega / 2\pi \quad (2)$$

We can sort out, as done in Sec. III, the carrier frequency ω_0 of the wave packet by letting

$$\rho(t, x) = \text{Re} A(t, x) \exp[-i\omega_0(t - x/c)] \quad (3)$$

The quantity $A(t, x)$ is the complex amplitude of the pulse envelope. We shall show that the pulse envelope at location x is then given by the following convolution integral in the time domain:

$$A(t, x) = e^{s_0 t'} \int_0^{t'} \frac{d}{du} [A(u) e^{s_0 u}] \Big|_{u=t'-t''} \times J_0(2\sqrt{\Lambda x t''}) dt'' \quad (4)$$

$A(t)$ is the initial envelope at $x=0$ corresponding to $\rho(\omega)$, $s_0 = i(\omega_0 - \omega_m) + 1/\tau$ is the complex frequency shift of the carrier wave from resonance, and $t' = t - x/c$ is the retarded time at location x . Equation (4) is quite a natural representation of $A(t, x)$, as it expresses the response of a linear and causal system to a given perturbation. It enables us to solve explicitly in Sec. IV the classic problem of Sommerfeld and Brillouin, namely the propagation of a truncated plane wave. It also yields asymptotic evaluations for short and long local times t' of signals with quite arbitrary initial envelopes which clearly show the time evolution of the received wave packet at location x . We thus obtain more precise definitions for precursors and the delayed signal than before. The delayed signal is found to propagate with a complex signal velocity, the real part of which is nothing but the classical group velocity. The imaginary part contributes to the pulse-shape distortion as it propagates. At the end of Sec. IV we consider bell-shaped pulses with no sharp front and show how this special case and how the analysis of Garrett and McCumber are included in our general result. In Sec. V we describe the experimental setup for our acoustic-pulse-propagation measurements in $^3\text{He-B}$ and the waveforms and the pulse velocities that we have observed. Our purpose is, in particular, to make explicit how the considerations of Secs. III and IV stem from actual laboratory observations. We present a summary of our findings on resonant pulse propagation in Sec. VI.

II. MODE CROSSING IN SUPERFLUID $^3\text{He-B}$ AND THE LORENTZ MODEL

The situation of mode crossing arising in superfluid $^3\text{He-B}$ which has motivated the present work may be described as follows.

The quantum liquid ^3He undergoes a transition to a superfluid state at a temperature below 2.7 mK.⁴⁷⁻⁴⁹ This state is characterized by an order parameter which describes the onset of the long-range order in momentum and spin space. This quantity is closely related to the quantum-mechanical wave function of the ground state. As the BCS pairing in ^3He takes place with orbital momentum $l=1$, the antisymmetry of the wave function under the exchange of two identical fermions imposes that

the spin part of the wave function be a triplet state. The full specification of the quantum state of the assembly of Cooper pairs requires three quantum numbers for the orbital part and three for the spin part. The order parameter is thus a 3×3 complex matrix. When this matrix is unity, it describes the Balian-Werthamer state which gives a good representation of superfluid ^3He in the B phase, i.e., the phase stable at temperatures well below the transition temperature T_c in the absence of applied magnetic field. This state corresponds to the most isotropic situation. In particular, the value of the pair-condensation energy, or gap parameter $\Delta(T)$, is constant over the Fermi surface.

We are concerned here with the propagation of sound in such a medium at temperatures sizably smaller than T_c where the gap parameter $\Delta(T)$ is well formed and the background of normal quasiparticles plays a minor role. In such a situation,⁵⁰ a low-frequency [$\hbar\omega \ll \Delta(T)$] sound wave propagates with very weak damping, its velocity being governed by molecular fields in much the same way as zero sound in normal liquid ^3He . At higher frequencies interesting features due to the internal structure of the order parameter occur. Among the 18 possible eigenmodes of the 3×3 complex matrix, the so-called pair-vibration modes, two groups, each with a fivefold degeneracy, couple to density fluctuations.⁵¹ This coupling gives rise to remarkable effects on the propagation of sound. Since the level degeneracy is not lifted in the situation that we shall be dealing with, we shall refer to these two groups as if they were single levels. Of these two modes, called the “squashing” and the “real squashing” modes after the shape of the distortion of the imaginary and the real components of the order parameter, the first is strongly coupled to density fluctuations while the second is only weakly coupled. Since damping is small in $^3\text{He-B}$ for $T < T_c$ as already mentioned, these modes are well defined. They give rise to well-marked attenuation peaks accompanied by large changes in the phase and group velocities, as shown for a typical situation in Fig. 1. Their study has been actively and fruitfully carried out in recent years⁵¹ as a way to probe the structure of the order parameter and to obtain quantitative information on the superfluid itself. They also offer a unique circumstance to study in a detailed and precise manner the general features of the propagation of signals in a high-homogeneity, low-dissipation resonant medium.

Our interest here lies primarily in these general features and we shall disregard the complications arising from a microscopic approach to the acoustic properties of $^3\text{He-B}$.⁵²⁻⁵⁴ In particular, as shown by Combescot,⁵⁴ the exact coupling between density fluctuations and the order parameter is of a quite particular and complicated nature. But, as will be shown below, the detailed form of the coupling disappears in the set of approximations that we shall have to make and it is quite sufficient to consider a simple phenomenological model along lines first sketched by Wölfle.^{55,56} In this model the density fluctuations ρ obey a wave equation and are coupled to a scalar quantity δ describing the amplitude of vibration of the internal modes. The equation of motion for δ reflects the basic properties of the pair-vibration mode under consideration,

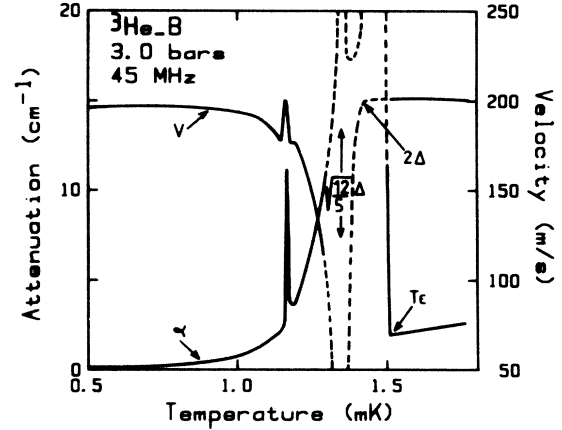


FIG. 1. Attenuation coefficient and group velocity of sound in superfluid $^3\text{He-B}$ at a pressure of 3.0 bars and a frequency of 45 MHz, vs temperature. The solid curves correspond to actual measurements, the dotted parts to extrapolation (compare with Fig. 13). At a temperature higher than T_c (~ 1.5 mK), i.e., in the normal Fermi liquid, the velocity is only very weakly dependent on temperature and α varies as T^2 . Immediately below T_c , the pair-breaking mechanism sets in and contributes strongly to the attenuation. The “squashing” mode occurs when the gap parameter $\Delta(T)$ becomes of the order of $\sqrt{5/12}\omega$. The attenuation is very high and the peak is not resolved. At lower temperature, when $\Delta(T) \sim \sqrt{5/8}\omega$, a smaller but sharply defined peak occurs which corresponds to the crossing of the sound mode and the “real squashing” mode.

namely its frequency ω_m and its propagation velocity c_m . It also includes dissipation through a relaxation time τ . For propagation in one dimension along x with velocity c_0 , these two coupled partial-differential equations are expressed by

$$\frac{\partial^2 \rho}{\partial t^2} + \frac{2}{\tau_0} \frac{\partial \rho}{\partial t} - c_0^2 \frac{\partial^2 \rho}{\partial x^2} = \gamma_0 \frac{\partial^2 \delta}{\partial x^2}, \quad (5)$$

$$\frac{\partial^2 \delta}{\partial t^2} + \frac{2}{\tau} \frac{\partial \delta}{\partial t} + \omega_m^2 \delta - c_m^2 \frac{\partial^2 \delta}{\partial x^2} = \gamma_m \frac{\partial^2 \rho}{\partial x^2}. \quad (6)$$

These equations refer to the propagation of sound in the collisionless regime, for a sound frequency such that $\omega\tau_0, \omega\tau \gg 1$. They can be derived from a simple Lagrangian density involving velocity-independent forces and they possess a well-behaved mechanical analog. They are well borne out by experiments on the transmission of sound⁵¹ and on the longitudinal-acoustic impedance.⁵⁷ It should, however, be noted that the simple form of the coupling terms in Eqs. (5) and (6) bears little relation to that suggested by the microscopic approach of the problem.⁵⁴ Also, the pair-vibration amplitude δ possesses different time-reversal properties for the squashing and the real squashing modes: In the case of the squashing mode, δ should be instead interpreted as a time derivative of the vibration amplitude. The above model, with the two parameters γ_0 and γ_m , must be considered purely

phenomenological. For simplicity, we shall neglect $1/\tau_0$, which gives rise to the small residual attenuation in the absence of modes.

This set of equations describes the crossing of two well-behaved modes with $c_0 > c_m$. Their unperturbed dispersion curves corresponding to plane waves propagating as $\exp[-i(\omega t - kx)]$ are shown in Fig. 2 and are expressed by

$$k_0^2 = \omega^2 / c_0^2, \tag{7}$$

$$k_m^2 = (\omega^2 - \omega_m^2 + 2i\omega/\tau) / c_m^2. \tag{8}$$

When the interaction $\Gamma = \gamma_0 \gamma_m / c_0^2 c_m^2$ is turned on, the energy levels are repelled, in agreement with the requirements of perturbation theory⁵⁸ provided that $\Gamma > 0$. The two branches of the dispersion curve in the coupled-mode case are given by

$$k^2 = \{k_m^2 + k_0^2 + [(k_m^2 - k_0^2)^2 + 4\Gamma k_m^2 k_0^2]^{1/2}\} / 2(1 - \Gamma). \tag{9}$$

When Γ becomes larger than 1, the behavior of the dispersion curve changes drastically. The excitation energy of the lower branch becomes negative. As it then costs no energy to create such an excitation, the system grows unstable against fluctuations. The stability of the system thus requires that

$$0 \leq \Gamma < 1. \tag{10}$$

If we let $z = k_m^2 / k_0^2$, k^2 is an analytic function of z with a pole at infinity and two branch points at

$$z_0 = 1 - 2\Gamma + 2[\Gamma(\Gamma - 1)]^{1/2}. \tag{11}$$

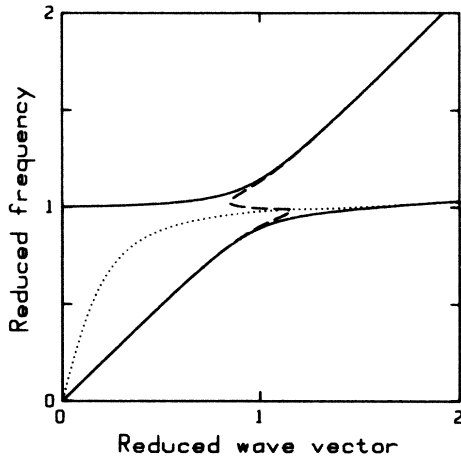


FIG. 2. Dispersion curve in a mode-crossing situation. The solid curves correspond to a strong mode coupling with no damping. The modes are repelled from one another and the upper and lower branches are well differentiated. When the collision time is decreased below a level specified by Eq. (12), the real part of the wave vector follows the dotted and dashed curves. The physical modes, i.e., the zero-sound and squashing modes in the case of $^3\text{He-B}$, remain identifiable. The Lorentzian approximation yields a good description of the zero-sound mode.

These branch points are located on the unit circle in the complex z plane. The function k^2 is double valued. The two determinations correspond to the two branches of the dispersion curves (Fig. 2). The root extraction from k^2 to k leads to waves traveling in opposite directions along x and does not elucidate any new physical information. We therefore study k^2 and choose the branch cut joining z_0 and z_0^* along the arc of unit circle going through $+1$, as shown in Fig. 3. When z varies along a path which crosses this cut, the determination of k^2 changes from one Riemann sheet to the other. According to this definition, the two Riemann sheets correspond to the zero-sound mode and pair-vibration mode, respectively. More specifically, if z varies along the real axis as in the case of vanishing damping ($1/\tau \rightarrow 0$), the branch determination changes, as pictured in Fig. 2, from zero sound to pair vibration. If the path is chosen in such a way as to avoid the cut, the original ($\Gamma = 0$) branch determination is preserved. As ω varies from 0 to ∞ , z describes a parabola from $-\infty$ to c_0^2/c_m^2 ($\gg 1$) crossing the imaginary axis at $2i(c_0^2/c_m^2)/\omega_m \tau$ for $\omega_0 = \omega_m$. The condition to remain on a given physical mode (or on a given Riemann sheet) is geometrically obvious. It is expressed analytically in an approximate way ($c_m^2/c_0^2 \ll 1$) by $\text{Im}z > \text{Im}z_0$ at $\text{Re}z = \text{Re}z_0$, or

$$\Gamma(1 - \Gamma) \frac{c_m^4}{c_0^4} (\omega_m \tau)^2 < 1. \tag{12}$$

Depending on the values of the parameters, we have two cases of markedly different physical behavior. Either

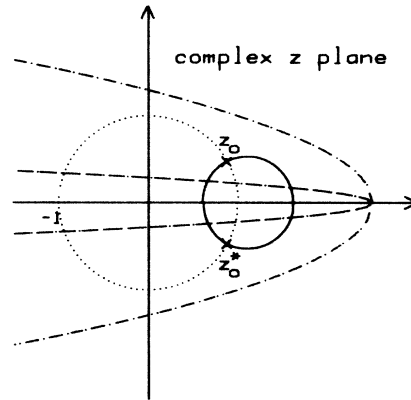


FIG. 3. Complex z plane. The dotted circle, of unit radius, is the locus of the branch points given by Eq. (11). For a given value of Γ (here 0.06), these branch points are located at z_0 and z_0^* . The branch cut joining these points may be taken as the area of unit circle going through $z = 1$. The dashed curves represent the parabolas defined by $z = k_m^2/k_0^2$, where k_0^2 and k_m^2 are given by Eqs. (7) and (8), when ω varies from $-\infty$ to $+\infty$. These parabolas cut the real axis for $\omega = 0$ at $z = c_0^2/c_m^2$. For large damping, the parabola (given by the dashed-dotted curve) does not cross the branch cut and the physical modes retain their identification. The dashed parabola crosses the cut between z_0 and z_0^* and remains on a given Riemann sheet. In this last case, the modes are strongly repelled and correspond to the solid curves in Fig. 2. The domain of convergence of the series given by Eq. (13) lies outside of the solid line quartic curve going through z_0 and z_0^* .

damping is small enough so that the modes are repelled and do not overlap, or it is large and causes level broadening and an actual crossing of the modes. An example in a physical system of the former case, total branch repulsion, is provided by the squashing mode. For instance, at 13.5 bars and 105 MHz with the parameters given in Ref. 57, we have $\Gamma=0.59$ and $\Gamma(1-\Gamma)(c_m^4/c_0^4)(\omega_m\tau)^2=425$. Condition (12) is strongly violated. Plots of the phase and group velocities and of the attenuation coefficient in such a case are given in Fig. 4. Pulse propagation occurs at the group velocity with negligible distortion, as is indeed observed experimentally and as will be reported in Sec. V.

The other situation where each mode retains its original identity is the more commonly met. This will be the case of the real squashing mode. It is amenable to a simple description due to Lorentz⁵⁹ which is obtained by expanding the square root in Eq. (9) in power series of $\xi=4\Gamma z/(1-z)^2$, with $\epsilon=\pm 1$:

$$k_\epsilon^2 = k_m^2 \frac{1+\epsilon}{2(1-\Gamma)} + k_0^2 \frac{1-\epsilon+2\epsilon\Gamma}{2(1-\Gamma)} + \epsilon \frac{\Gamma}{(1-\Gamma)} \frac{k_0^4}{k_m^2 - k_0^2} + \dots \quad (13)$$

The domain of convergence of this series, defined by $|\xi| < 1$, is delimited by a closed quartic curve in the z plane, going through the branch points z_0 and z_0^* . When Γ is small, this curve is close to the circle of radius $2\Gamma^{1/2}$ centered on $z=1$. Outside of this domain, the series con-

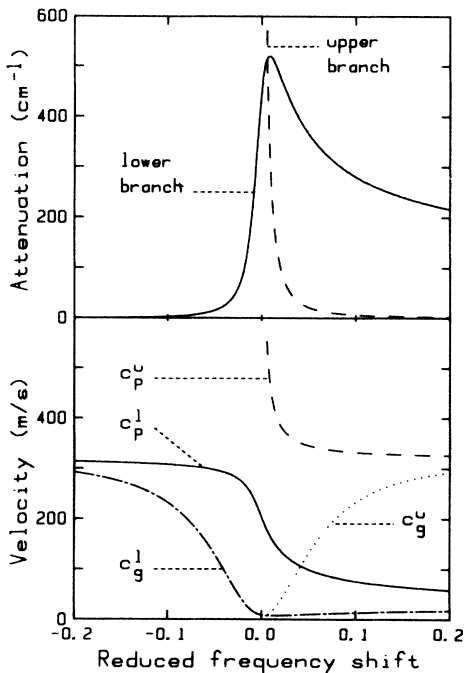


FIG. 4. Attenuation coefficient (top), and phase and group velocities vs reduced frequency shift $\Delta\omega/\omega_m$ in the case of strong mode repulsion. $c_p^{u(l)}$ refer to the phase (group) velocities of the upper (lower) branches. This figure corresponds to the actual case of superfluid $^3\text{He-B}$ at 13.5 bars and 105 MHz with the parameters of Ref. 57 ($\Gamma=0.59$, $\tau=2.5 \mu\text{s}$, $c_m/c_0=0.16$). Group velocities are computed as $\text{Re}(\partial\omega/\partial k)$.

verges. It is represented to fair accuracy by its terms up to first order, namely

$$k_+^2 = k_m^2 \left[1 + \frac{\Gamma}{1-\Gamma} \frac{k_m^2}{k_m^2 - k_0^2} \right], \quad (14)$$

$$k_-^2 = k_0^2 \left[1 - \frac{\Gamma}{1-\Gamma} \frac{k_0^2}{k_m^2 - k_0^2} \right], \quad (15)$$

only when $|4\Gamma z/(1-z)^2|$ is much smaller than 1. This condition is fulfilled whenever

$$4\sqrt{3}\Gamma/|z| \ll 1. \quad (16)$$

When this last inequality holds and if Γ is not too close to 1, i.e., $\Gamma < 1 - \sqrt{3}/12$, the zero-sound branch ($\epsilon=-1$) can be further expanded. Letting

$$a = 1 - \frac{\omega_m^2}{\omega^2} - \frac{c_m^2}{c_0^2}, \quad (17)$$

$$b = 2/\omega\tau, \quad (18)$$

$$\lambda = \frac{\Gamma}{2(1-\Gamma)} \frac{c_m^2}{c_0^2}, \quad (19)$$

we find

$$k = \frac{\omega}{c_0} \left[1 - \frac{\lambda}{a+ib} \right]. \quad (20)$$

The phase velocity c_p and the attenuation coefficient α , which are such that $k = \omega/c_p + i\alpha$, are then given by the following well-known formulas:

$$c_0/c_p = 1 - \lambda a/(a^2 + b^2), \quad (21)$$

$$\alpha = (\lambda\omega/c_0)b/(a^2 + b^2). \quad (22)$$

Equations (21) and (22) describe the Lorentzian dispersion and absorption line shapes.⁶⁰ The Lorentzian approximation is valid, strictly speaking, only under condition (16), which we may rewrite as⁶¹

$$\lambda\omega_m\tau \ll 1. \quad (23)$$

The Lorentzian approximation is also expected to yield qualitatively correct results under the less restrictive condition (12), that is, as long as modes retain their original identity. We speculate that this same remark will also apply to our analysis of pulse propagation in a resonant medium which makes use of the simplified expression (20) for the wave vector. Arguments to justify this point will be presented below. The case of strong mode repulsion which corresponds to the squashing mode at $T \ll T_c$ will be briefly considered in Sec. VI.

III. THE SLOWLY VARYING ENVELOPE APPROXIMATION

In this section, in order to put the problem of the propagation of pulses in a resonant medium in a fully tractable form, we further simplify our description beyond the Lorentzian approximation. We follow a method originally due to McCall and Hahn³³ to deal with the nonlinear propagation of waves of strong amplitude in a resonant

medium and used by a number of authors^{35,37,23} in the linear case as well. This method, the slowly varying envelope approximation, has common roots with the centering method used in the theory of nonlinear oscillations.⁶² It takes advantage of the two following facts.

(1) The light or sound pulse traveling in the resonant medium is, in practical situations, a wave packet of finite and rather small spectral width, that is, a carrier wave at frequency $\omega_0/2\pi$ on which is impressed a slowly varying amplitude and frequency modulation.

(2) The medium is homogeneous and extends to infinity in the direction of propagation so that there are no back-scattered waves. The wave packet travels with a phase velocity which is close to $+c_0$. Under these conditions, if we let, as in Eq. (3),

$$\rho(t,x) = \text{Re}A(t,x)\exp[-i\omega_0(t-x/c_0)], \quad (24)$$

where A is a complex amplitude describing the pulse envelope, this amplitude will vary slowly in space and time. The following inequalities,

$$\left| \frac{\partial A}{\partial t} \right| \ll \omega_0 |A|, \quad \left| \frac{\partial A}{\partial x} \right| \ll \omega_0 |A|/c_0, \quad (25)$$

hold so that the second order partial-differential equations (5) and (6) can be reduced to first-order equations. This simplified but approximate set can then be solved as is done in the Appendix to obtain the time and space evolution of the pulse envelope.

We take below a simpler and more economical approach starting from the Fourier representation of the exact solution given by Eq. (2) and pertaining to a wave propagating with wave vector k_+ in the medium initially at rest:

$$\rho(t,x) = \int_{-\infty}^{+\infty} \rho(\omega) e^{-i(\omega t - k_+ x)} \frac{d\omega}{2\pi}. \quad (26)$$

In the Lorentzian approximation the wave vector of the zero-sound branch will be given by Eq. (20). The quantity

$$\begin{aligned} \rho(t,x) &= \int_{-\infty}^0 A^*(-\omega - \omega_0) e^{-i(\omega t - k_+ x)} \frac{d\omega}{2\pi} + \int_0^{+\infty} A(\omega - \omega_0) e^{-i(\omega t - k_+ x)} \frac{d\omega}{2\pi} \\ &= \text{Re} e^{-i\omega_0(t-x/c_0)} \int_{-\infty}^{+\infty} A(\Omega) \exp \left[-i\Omega t + i \left[k_+(\omega_0 + \Omega) - \frac{\omega_0}{c_0} \right] x \right] \frac{d\Omega}{2\pi}. \end{aligned} \quad (32)$$

The last equality describes the propagation of the complex envelope, i.e., of the amplitude and phase modulation, according to

$$A(t,x) = \int_{-\infty}^{+\infty} A(\Omega) e^{-i(\Omega t - K_+ x)} \frac{d\Omega}{2\pi}, \quad (33)$$

with a wave vector given by the following relation:

$$K_+(\omega_0, \Omega) = k_+(\omega_0 + \Omega) - \omega_0/c_0. \quad (34)$$

For a cw signal of unity amplitude, $A(\Omega)$ is a Dirac δ function. We find, by setting $\Omega=0$ in Eq. (33) that the full continuous wave propagates with a complex phase velocity $c_p = \omega_0/k_+(\omega_0)$, as expected. For a modulation at finite but sufficiently small frequency Ω , we recover the usual expression for the complex group velocity:

$\rho(\omega)$ is the Fourier transform of the density fluctuations at $x=0$ which are given as an initial condition:

$$\rho(\omega) = \int_{-\infty}^{+\infty} \rho(t, x=0) e^{i\omega t} dt. \quad (27)$$

As $\rho(t,x)$ is a real quantity, we have the following symmetry properties:

$$\rho^*(\omega) = \rho(-\omega), \quad (28)$$

$$k^*(\omega) = -k(-\omega). \quad (29)$$

From the definitions of the envelope $A(t,x)$ and its Fourier transform $A(\omega)$, we readily obtain the following relation:

$$\rho(\omega) = A(\omega - \omega_0) + A^*(-\omega - \omega_0). \quad (30)$$

Let us now make use of the assumption that $A(t)$ is a slowly varying function of time, or, more precisely, that its Fourier transform has a bounded spectrum, that is, $A(\Omega)=0$ if $|\Omega| \geq \Omega_p$ with $\Omega_p < \omega_0$. With this bandwidth restriction, it is then clear that the following relations hold:

$$\rho = \begin{cases} A(\omega - \omega_0) & \text{for } \omega > 0, \\ A^*(-\omega - \omega_0) & \text{for } \omega < 0. \end{cases} \quad (31)$$

These relations mean physically that the spectrum of $\rho(\omega)$ is peaked about ω_0 and $-\omega_0$ and that these frequencies can be heterodyned to low frequencies with insignificant loss of information. This statement is a mere translation of an assumption which is implicit in the very definition of a wave packet. We can also take a more down-to-earth point of view. In an actual experiment the observation bandwidth is limited by instruments; only a part of the spectrum is sampled and recorded. Condition (31) then yields a better representation of real-world signals than the mathematically exact solution (2). Let us carry out this operation in Eq. (26) by making use of Eqs. (30), (31), and (29):

$$\frac{1}{c_g} = \frac{\partial K_+}{\partial \Omega} \Big|_{\Omega=0} = \frac{\partial k_+}{\partial \omega_0}. \quad (35)$$

As we have mentioned above, Eq. (33) is hardly an approximation and can actually be considered as a more appropriate description of actual experimental situations than Eq. (2). It yields perfectly well-behaved results for the phase and group velocities. It is also much easier to evaluate numerically, as $A(t)$ is a slowly varying function of time. It provides the starting point for our computer simulations.

To proceed with the analytical approach, we replace $k_+(\omega)$ by its Lorentzian form (20) in expression (34). We then use the fact that $A(t)$ has a bounded spectrum to expand the denominator in Ω/ω_0 :

$$K_+ = \frac{\Omega}{c_0} - \frac{\lambda\omega_0}{c_0} \frac{1 + \Omega/\omega_0}{(a + ib)(1 - 2\Omega/\omega_0) + 2\Omega(1 - c_m^2/c_0^2 + ib/2)/\omega_0} \tag{36}$$

Two situations may arise.

Either $a + ib$ is not small and the expansion in Ω/ω_0 can be carried further with little loss of accuracy. This leads to the following expression for the group velocity, which is valid in any region of the dispersion curve smooth on a scale set by Ω_P :

$$\frac{1}{c_g} = \frac{1}{c_0} \left[1 + 2\lambda \frac{1 - c_m^2/c_0^2 - 3a/2 - ib}{(a + ib)^2} \right] \tag{37}$$

Equation (37) is completely equivalent to Eq. (35).

Or else, we are close to a resonance with a Lorentzian line shape in which case $a + ib$ is not large with respect to Ω/ω_0 . The leading term in the expression for K_+ is then

$$K_+ = \frac{\Omega}{c_0} - \frac{\lambda\omega_0}{c_0} \frac{1}{a + ib + 2\Omega/\omega_0} \tag{38}$$

The pole at

$$\Omega_0 = \omega_0(a + ib)/2 \simeq -\Delta\omega + i/\tau$$

with $\Delta\omega = \omega_m - \omega_0$ clearly gives a much better representation of the anomalous dispersion region than the series expansion leading to Eq. (37). We therefore expect that the propagation of a pulse with a spectrum of finite width will be more accurately described by the following expression for its envelope,

$$A(t, x) = \int_{-\infty}^{+\infty} A(\Omega) \exp \left[-i \left(\Omega(t - x/c_0) - \frac{\Lambda x}{\Delta\omega - i/\tau - \Omega} \right) \right] \frac{d\Omega}{2\pi} \tag{39}$$

than by the group velocity as conventionally derived. The coupling constant Λ is defined as

$$\Lambda = \lambda\omega_0^2/2c_0 = \alpha_m/\tau \tag{40}$$

where α_m is the peak amplitude attenuation in the cw regime.

As we shall now show, Eq. (39) is tractable analytically. This tradeoff justifies the approximations leading to Eq. (38) and the loss of accuracy that they entail. We shall refer to this set of approximations as the slowly varying envelope approximation because in its more commonplace version^{6,23,35,63} derived in the Appendix it leads to the same approximate dispersion relation, i.e.,

$$k = \frac{\omega}{c_0} - \frac{\Lambda}{\omega - \omega_m + i/\tau} \tag{41}$$

The general form of this relation, which appears as a single-pole propagator, is physically appealing and has been used without further justification by a number of authors.^{19,29,64} We have gone to great lengths to show that this form is implied by Eqs. (23) and (31), that is, a well-defined wave packet on a well-defined sound mode. Arguments are presented in the Appendix to extend its validity beyond the Lorentzian approximation. They amount to saying that the gross features of the propagation of a wide spectrum pulse, characterized by a time $\tau_P \approx 1/2\Omega_P$, will not be much affected by the relatively narrow stop band which develops in the dispersion curve in the strong-repulsion regime as long as

$$\lambda\omega_m\tau_P \ll 1 \tag{42}$$

Condition (42) replaces Eq. (23) when the latter breaks down: not so slowly varying pulses still propagate according to (41) when the Lorentzian approximation does not apply to plane waves anymore.

A serious shortcoming of Eq. (41) is that the limits $\omega \rightarrow 0$ and $\omega \rightarrow \infty$ are poorly represented because the frequency dependence of the coupling constant has been treated in a rather cavalier way. A proper behavior can be restored at least in part, as will be done below, by reintroducing a weak frequency dependence in Λ and τ .

We now turn to the integration of Eq. (39) which appears under the form of the inverse complex Fourier transform with respect to the local time $t' = t - x/c$ of the product of two functions, $A(\Omega)$ and

$$G(\Omega) = \exp[i\Lambda x / (\Delta\omega - i/\tau - \Omega)]$$

Let us set $s = i\Omega$, $s_0 = i\Delta\omega + 1/\tau$, and switch to Laplace transforms, which are better suited to initial value problems.³ The envelope $A(t, x)$ will be given by the time-convolution product of the two Laplace-inverse functions of $A(s)$ and $G(s)$. The inverse of $A(s)$ is nothing but $A(t)$, the initial signal envelope at $x = 0$. Knowing⁶⁵ that the transform of the Bessel function of order zero, $J_0(2\sqrt{\mu t})$, is $\exp(-\mu/s)/s$, the inverse transform of $G(s)$ can easily be shown to be

$$G(t) = e^{-s_0 t} \frac{d}{dt} [J_0(2\sqrt{\Lambda x t}) U_+(t)] \tag{43}$$

where $U_+(t)$ is the unit impulse (U_+ is zero at $t = 0$ and unity for $t > 0$). The time evolution of the complex envelope at x is therefore expressed by

$$A(t, x) = \int_0^{t'} A(t' - t'') e^{-s_0 t''} \frac{d}{dt''} \times [J_0(2\sqrt{\Lambda x t''}) U_+(t'')] dt'' \tag{44}$$

Equation (44) can also be written, after integrating by parts, in the form

$$A(t, x) = \int_0^{t'} \left[\frac{d}{dt'} A(t' - t'') + s_0 A(t' - t'') \right] \times e^{-s_0 t''} J_0(2\sqrt{\Lambda x t''}) dt'' . \quad (45)$$

As before, $t' = t - x/c_0$, $s_0 = i\Delta\omega + 1/\tau$, $\Delta\omega = \omega_m - \omega_0$, and $\Lambda = \lambda\omega_0^2/2c_0$. These time-convolution integrals express the linear response at x of the resonant medium to an input perturbation $A(t)$ at the origin. As expected, these integrals represent a causal signal, the fastest propagation velocity being at most equal to c_0 . They provide a time-domain representation of $A(t, x)$ and open the way to rather straightforward derivations of signal wave forms in a variety of cases.

IV. DELAYED SIGNAL AND PRECURSORS

This section contains the analytical results that we have obtained from the time-convolution representation (44) or (45) of the signal envelope $A(t, x)$. We shall consider first a few special input signals $A(t)$ before giving an asymptotic evaluation of the response for arbitrary signals.

A. Propagation of short pulses

If $A(t)$, within the restrictions expressed by Eqs. (25) or (31), can nevertheless be approximated as a Dirac pulse, i.e., if it is sharply peaked in time compared to the Bessel and the exponential functions but still contains many periods of the carrier wave, then Eq. (44) yields immediately

$$A(t, x) = e^{-s_0 t'} \left[\delta_+(t') + \left[\frac{\Lambda x}{t'} \right]^{1/2} J_{-1}(2\sqrt{\Lambda x t'}) U_+(t') \right] . \quad (46)$$

The sharp peak propagates undistorted at velocity c_0 and an oscillating tail develops. This tail is small and slowly varying at small x . It grows relative to the main signal and oscillates more rapidly with distance until the slowly varying envelope approximation fails. These features of propagation of short pulses, namely the propagation of a

$$A(t, x) = e^{-\Lambda x/s_0} + e^{-s_0 t'} [J_0(2\sqrt{\Lambda x t'}) + V_0(-2is_0 t', 2\sqrt{\Lambda x t'}) - iV_1(-2is_0 t', 2\sqrt{\Lambda x t'})] , \quad (51)$$

or, using the expansions of V_0 and V_1 in terms of Bessel functions,⁶⁶

$$A(t, x) = e^{-s_0 t'} \sum_{n=0}^{\infty} \left[s_0 \left[\frac{t'}{\Lambda x} \right]^{1/2} \right]^n J_n(2\sqrt{\Lambda x t'}) \quad (52)$$

$$= e^{-\Lambda x/s_0} - e^{-s_0 t'} \sum_{n=1}^{\infty} \left[-\frac{1}{s_0} \left[\frac{\Lambda x}{t'} \right]^{1/2} \right]^n \times J_n(2\sqrt{\Lambda x t'}) . \quad (53)$$

At long times the signal settles to its cw steady-state

transient at velocity c_0 and the formation of a wiggling response, constitutes general features that we shall meet again for other initial pulse shapes. The oscillatory tail formation described by Eq. (46) has been observed qualitatively in a number of experiments.^{26,39,44}

B. Propagation of a step input

The problem of the propagation of a signal which begins by a sharp front and settles to a steady-state regime for a sizable lapse of time has been considered, as mentioned in the Introduction, first by Sommerfeld,¹⁰ Brillouin,¹¹ and Baerwald¹² in connection with the question of the signal velocity. The step input was later also studied in the context of the self-induced transparency effect by Crisp^{35,36} and Hopf *et al.*³⁷ This problem is amenable to an exact analytical treatment as follows. If the initial envelope is a unit step function with a sharp front, the signal at x , given by Eq. (45), takes the following form:

$$A(t, x) = e^{-s_0 t'} J_0(2\sqrt{\Lambda x t'}) + s_0 \int_0^{t'} e^{-s_0 t''} J_0(2\sqrt{\Lambda x t''}) dt'' . \quad (47)$$

Using once again the equality,⁶⁵

$$\int_0^{\infty} e^{-y t} J_0(2\sqrt{\mu t}) dt = \frac{1}{y} e^{-\mu/y} , \quad (48)$$

we can write Eq. (47) in the following form:

$$A(t, x) = e^{-\Lambda x/s_0} + e^{-s_0 t'} J_0(2\sqrt{\Lambda x t'}) - s_0 \int_{t'}^{\infty} e^{-s_0 t''} J_0(2\sqrt{\Lambda x t''}) dt'' . \quad (49)$$

The first term of this last equation is the steady-state response and the second term the dominant short-time part of the wiggling response. The last integral may be evaluated in closed form, using a relationship involving Lommel's functions,⁶⁶

$$w e^{iw/2} \int_1^{\infty} J_0(zt) e^{-i(wt^2/2)} t dt = V_1(w, z) + iV_0(w, z) . \quad (50)$$

The response at x to a step excitation takes the following closed form:

value, $\exp(-\Lambda x/s_0)$. At short times it behaves as $J_0(2\sqrt{\Lambda x t'})$, that is, its front is heavily distorted but suffers little attenuation. In other words, Beer's law, according to which the propagating wave is attenuated exponentially with distance, is obeyed only by the long-term part of the response. The separation between free and forced oscillations, i.e., short- and long-time responses, is made in a quite explicit manner. This behavior is illustrated in Fig. 5, obtained by direct evaluation of the Fourier integral (33) for a rectangular input pulse. On resonance and for vanishing damping, a situation in which the Lorentzian approximation is not valid, Eq. (52) is identical to a result already given by Crisp³⁵ and, prior

to him, by Shiren¹⁹ and later by Yablonovitch and Goldhar.⁴⁰ The typical pattern developed by the response has been called a “zero π ” pulse in reference to the area theorem, as recalled in the Introduction. However, the application of this theorem to pulses of small area does not carry the same weight and usefulness as in the case of 2π and higher topological charge solitons. Furthermore, 0π pulses will be shown below to belong to the more general class of precursors, introduced by Brillouin and Sommerfeld. We shall refer to them in the following as “resonant precursors.”

In Eq. (53) we see that the wiggling precursory motion has decayed to the level of the steady-state response when the modulus of $\exp(\Lambda x/s_0 - s_0 t')$ has decreased to unity, that is, at a time t'_A such that

$$t'_A = \frac{\Lambda x}{(\Delta\omega)^2 + 1/\tau^2}. \quad (54)$$

If this last condition (which expresses the time at which the delayed long-term signal can be observed above the precursor motion) was taken as a definition of the signal arrival time, the signal velocity would be given by

$$\frac{1}{c_e} = \frac{1}{c_0} + \frac{\Lambda}{(\Delta\omega)^2 + 1/\tau^2}. \quad (55)$$

This expression is identical to Baerwald's result,¹² which has now been obtained in a very direct manner. However, this result will not correspond to the signal velocity derived below. The reason for this discrepancy will become apparent later, but stems from a different definition of the signal and of its time of arrival. It may well be, and will be shown to be indeed so, that signals and precursors overlap in such a way as to render the condition leading to the definition of t'_A given by Eq. (54) inappropriate. This can already be guessed from Fig. 5, where the delayed signal can clearly be identified in the three top snapshots of the pulse arrival at x , but not anymore in the fourth, in which the carrier frequency is much closer to resonance. In this case it is clear that the visible part of the response is solely due to transients. Equation (55) yields, in fact, the velocity of energy propagation in steady state, as shown convincingly by Loudon⁶⁷ and others.^{9,15} To clarify the concept of signal velocity, we need a way to separate in a more satisfactory manner the precursory response, the “fluchtig” part in Baerwald's words, from the “signal” itself. This will be done in the next section.

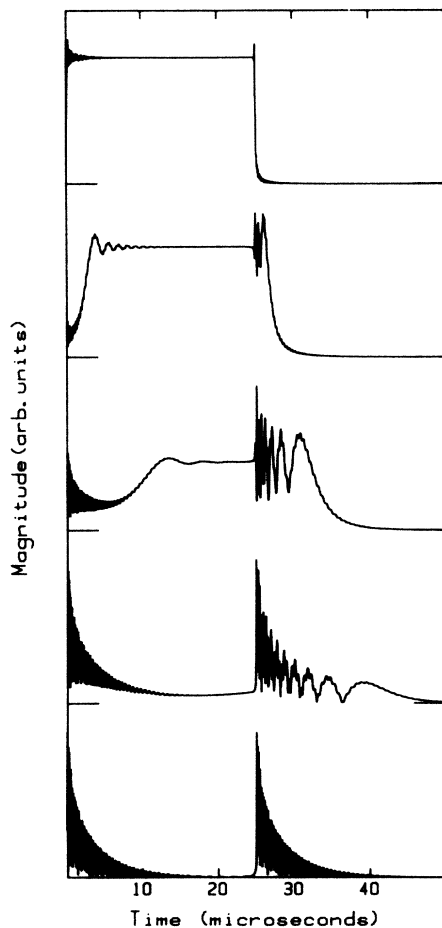


FIG. 5. Envelope of the received signal corresponding to a step input vs time. The duration of the initial rectangular signal amplitude is $\tau_{rf} = 25 \mu\text{s}$. The medium parameters are $\lambda = 10^{-2}$, $\tau = 5 \mu\text{s}$, $c_0 = 310 \text{ m/s}$. The frequency at resonance is 45 MHz, the sound flight path 0.025 cm. The top curve corresponds to a frequency far off resonance, the bottom curve to the resonance frequency. From top to bottom, the frequency shifts from resonance $\Delta\omega$ are, in 10^6 rad/s , 50, 12, 6, 4, and 0, and the plotted amplitudes are multiplied by 1, 1.33, 3.22, 5.75, and 5.77, respectively. Both the delayed signal and the transient response are clearly visible on the middle curve. Far from resonance, the signal is virtually undistorted; on resonance, the transients dominate the response.

C. Slowly varying signals: The delayed signal and its velocity

We now wish to obtain an asymptotic evaluation, valid at large Λx , of the time-convolution integral in Eq. (45) for slowly varying initial envelopes $A(t)$. Guided by the previous discussion, we look for the formation of a delayed signal at local times t' which are not small. We can then take an asymptotic representation of $J_0(z)$ for large positive values of the argument:⁶⁶

$$J_0(z) = \left[\frac{2}{\pi z} \right]^{1/2} \left[\cos \left[z - \frac{\pi}{4} \right] + \frac{1}{8z} \sin \left[z - \frac{\pi}{4} \right] + \dots \right]. \quad (56)$$

The estimated error in this asymptotic representation is of the order of the first neglected term. Thus, as soon as the argument becomes of the order of 3 or larger, J_0 can be replaced in Eq. (45) by the cosine term. If we define θ as the time at which this representation of J_0 becomes adequate for our purpose, $\theta \sim 9/4\Lambda x$, the integral from 0 to t' in Eq. (45) can be split into a short-time part I_s , from 0 to θ , and a long-time part I_l , from θ to t' .

We shall consider the long-time integral I_l first. Because Λx has been assumed large, it is amenable to a simple asymptotic expansion. If we let $t'' = \Lambda x u^2$, it becomes

$$I_l = \left[\frac{\Lambda x}{\pi} \right]^{1/2} \int_{(\theta/\Lambda x)^{1/2}}^{(t'/\Lambda x)^{1/2}} \left[\frac{dA}{dt} + s_0 A \right] \Big|_{t' - \Lambda x u^2} \left[\exp \left[-i\epsilon \frac{\pi}{4} - \Lambda x (2i\epsilon u - s_0 u^2) \right] + (\text{idem with } \epsilon = -1) \right] u^{1/2} du, \quad (57)$$

which is the sum of two integrals ($\epsilon = \pm 1$) of the form

$$\int_{u_1}^{u_2} g(u) e^{\kappa h(u)} du.$$

These integrals can be evaluated, in the limit $\kappa = \Lambda x \rightarrow \infty$, by the saddle-point method.⁶⁸⁻⁷¹ With $h(u) = -s_0 u^2 + 2i\epsilon u$, the saddle points, defined by $h'(u_0) = 0$, are located at $u_0 = i\epsilon/s_0$. As $h''(u_0) = -2s_0$ is different from zero, and assuming that

$$\frac{dA}{dt} + s_0 A$$

does not become singular in the vicinity of the saddle points, the contribution to the integral (57) of the integration path in the vicinity of the saddle point is given by

$$\begin{aligned} \left[\frac{-\pi}{2\kappa h''(u_0)} \right]^{1/2} g(u_0) e^{\kappa h(u_0)} &= \left[\frac{\Lambda x}{\pi} \right]^{1/2} \left[\frac{dA(t)}{dt} + s_0 A(t) \right] \Big|_{t=t'+\Lambda x/s_0^2} \left[\frac{i\epsilon\pi}{4s_0^2\Lambda x} e^{-i\epsilon(\pi/2)} \right]^{1/2} e^{-\Lambda x/s_0} \\ &= \frac{1}{2s_0} \left[\frac{dA(t)}{dt} + s_0 A(t) \right] \Big|_{t=t'+\Lambda x/s_0^2} e^{-\Lambda x/s_0}. \end{aligned} \quad (58)$$

Assuming that the endpoints of the integration interval yield no pathological contributions, Eq. (58) represents the asymptotic evaluation of the integral (57) with $\epsilon = 1$. Adding the integral with $\epsilon = -1$, we arrive at the following expression for the long-time part of the signal:

$$A(t, x) = \left[A(u) + \frac{1}{i\Delta\omega + 1/\tau} \frac{d}{du} A(u) \right] \Big|_{u=t'+\Lambda x/(i\Delta\omega + 1/\tau)^2} \exp[-\Lambda x/(i\Delta\omega + 1/\tau)]. \quad (59)$$

Equation (59) is the first main result of this subsection and describes the "delayed" signal for a large class of input signals.

For quasistationary inputs ($dA/dt \sim 0$), Eq. (59) reduces to the following form,

$$A(t, x) = A(t - x/c_s) \exp \left[-\alpha x + ix \left[\frac{1}{c_p} - \frac{1}{c_0} \right] \omega_0 t \right],$$

with

$$\alpha = \Lambda\tau/[1 + (\Delta\omega\tau)^2], \quad (60)$$

$$\frac{1}{c_p} = \frac{1}{c_0} + \frac{\Lambda}{\omega_0} \frac{\tau^2 \Delta\omega}{1 + (\Delta\omega\tau)^2}, \quad (61)$$

$$\frac{1}{c_s} = \frac{1}{c_0} + \frac{\Lambda}{(i\Delta\omega + 1/\tau)^2}. \quad (62)$$

The quantities α and c_p are the attenuation coefficient and the phase velocity of the carrier wave. They correspond, as expected, to the expressions given by Eqs. (21) and (22) for the Lorentzian line shape.

The quantity c_s , given by Eq. (62), is the complex signal velocity. It describes the propagation velocity and the attenuation of the slowly varying modulation in a manner exactly similar to that with which the complex phase velocity describes the alteration of the carrier wave. Its real part, the velocity of the signal envelope, is expressed by

$$\frac{1}{c'_s} = \frac{1}{c_0} + \Lambda \frac{(\Delta\omega)^2 - 1/\tau^2}{[(\Delta\omega)^2 + 1/\tau^2]^2}. \quad (63)$$

Its imaginary part yields the group attenuation coefficient:

$$\alpha_g = 2\Lambda\Delta\omega\tau^3\omega_0/[1 + (\Delta\omega\tau)^2]^2. \quad (64)$$

As can readily be seen for a harmonic modulation at frequency Ω , $A(t) = A_0 + A_1 \exp(i\Omega t)$, the group attenuation coefficient is nothing but the difference of attenuation between the carrier wave and the side band arising from the modulation.

The full asymptotic result (59) is liable to unambiguous interpretation since the functional form of the signal is well defined if not conserved. It includes two contributions which are going to distort its shape.

(1) The derivative $(dA/dt)/(i\Delta\omega + 1/\tau)$ evaluated at the signal velocity.

(2) The imaginary part of the signal velocity. As long as this imaginary part is small, we may expand A in series,

$$A(z' + iz'') = A(z') + iz'' \frac{dA(z')}{dz},$$

with $z'' = -\alpha_g x/\omega_0$.

Both corrections involve dA/dt and are of the same form. It is clear that, within the range of validity of the Lorentzian and of the slowly varying envelope approximations, these corrections are not very large. Thus the concept of complex signal velocity, already put forward by Johnson,³⁰ leads to no difficulties of interpretation. Its usefulness lies in the fact that it produces an analytical formula which, albeit approximate, describes the propaga-

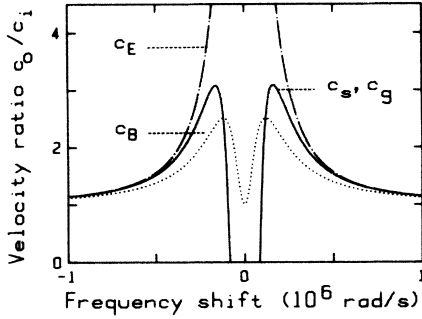


FIG. 6. Inverse velocities normalized to c_0 vs $\Delta\omega$ for the energy velocity c_E [Eq. (55)], the signal velocity c_s [Eq. (64)], the group velocity c_g [Eq. (37)], and Brillouin's signal velocity c_B [Eq. (65)]. These velocities are computed in the realistic case of the "real squashing" mode in $^3\text{He-B}$ at 1.2 bars and 45 MHz, for which, according to Ref. 6, $\Lambda=0.146$, $\tau=10.7 \mu\text{s}$, $c_0=202$ m/s.

tion of signals in a region of anomalous dispersion in a reasonably well-founded way. This description is notably different from that provided by Baerwald's approach and represented by Eq. (55). It is much closer to the classical group-velocity picture. A comparison between group and signal velocities, given by Eqs. (37) and (63), respectively, is shown in Fig. 6. The difference between these two quantities, which cannot be distinguished on the graph, is indeed very small. It may, in fact, not be larger than the inaccuracies introduced by the envelope approximation itself.

Brillouin's signal velocity is also shown in Fig. 6. It is defined¹ by geometrical considerations in the ω_- complex plane from the time at which the path of steepest descent coming down from the saddle point reaches the point of the real axis corresponding to the excitation frequency ω_0 . The envelope approximation simplifies, notably, Brillouin's geometrical arguments and leads to the following analytical expression for this author's signal velocity:

$$\frac{1}{c_B} = \frac{1}{c_0} + \Lambda \frac{(\Delta\omega)^2}{[(\Delta\omega)^2 + 1/\tau^2] \{1/\tau + [(\Delta\omega)^2 + 1/\tau^2]^{1/2}\}^2}. \quad (65)$$

Again, the behavior of c_B is rather different from that of c_g .

Thus, the second main result obtained in this subsection is an extension in the anomalous dispersion region of the validity of the classical concept of group velocity to signals with rise and fall times which are neither extremely long nor short. For the former case, this validity is well established. For the latter, meaningful events occur at time smaller than θ . We therefore need to consider the short-time part, I_s , of the signal.

D. The precursors

To proceed with the evaluation of the short-time part of the signal, that is, the very front of the wave packet, we need to tackle integral (45) without taking the asymptotic approximation of the Bessel function J_0 . We use instead

the fact that neither J_0 nor the exponential of $-s_0 t$ vary rapidly with respect to $A(t)$ for small values of t . The expansion of integral (45) at small local times is obtained by carrying out successive integration by parts.⁷⁰ If the integral

$$J = \int_{u_1}^{u_2} g(u)h(u)du$$

is such that g is N times continuously differentiable and h is integrable, then it can be expressed by

$$J = \sum_{n=0}^{N-1} s_n + \mathcal{R}_n,$$

$$s_n = (-1)^n [g_n(u_2)h_{-n-1}(u_2) - g_n(u_1)h_{-n-1}(u_1)],$$

$$\mathcal{R}_n = (-1)^n \int_{u_1}^{u_2} g_n(u)h_{-n}(u)du,$$

where g_n is the n th derivative of g , and h_{-n} the n th repeated integral of h . Applying this formula with

$$g(t'') = \left[\frac{d}{dt'} A(t' - t'') + s_0 A(t' - t'') \right] e^{-s_0 t''},$$

$$g_n(t'') = (-1)^n \frac{d^{n+1}}{du^{n+1}} \left[A(u)e^{s_0 u} \right] \Big|_{u=t'-t''} e^{-s_0 t''},$$

$$h(t'') = J_0(2\sqrt{\Lambda x t''}),$$

$$h_{-n}(t'') = \left[\frac{t''}{\Lambda x} \right]^{n/2} J_n(2\sqrt{\Lambda x t''}),$$

we arrive, using the fact that $A(t=0)=0$ and assuming $A(u)$ to be $N+1$ times continuously differentiable in the interval $(0, t')$, at the following asymptotic expansion of the contribution to the response of the $t'=0$ endpoint of Eq. (45):

$$A(t, x) = e^{-s_0 t'} \sum_{n=1}^N \left[\frac{d^n}{du^n} [A(u)e^{s_0 u}] \Big|_{u=0} \left[\frac{t'}{\Lambda x} \right]^{n/2} \times J_n(2\sqrt{\Lambda x t'}) \right]. \quad (66)$$

Whenever the magnitude of this short-time response becomes comparable to (or, *a fortiori*, larger than) the contribution of the saddle points expressed by Eq. (59), it has to be taken into account. For instance, let us consider the response as given by Eq. (66) at short distance x and short local time ($t' \ll 1/\Lambda x$). We can replace the Bessel functions by their small argument expansions, $J_n(z) \sim z^n/(2^n n!)$. Then, Eq. (66) reduces to the Taylor expansion of $A(t)$ at small t' . This expansion has a very restricted range of validity, except at very small x (i.e., close to the origin), but it shows how the general result expressed by Eq. (45) merges into the initial condition at $x=0$.

At larger distance the Bessel functions take on their oscillatory behavior more rapidly, the signal delay builds up, and the short-time response expressed by Eq. (66) describes a transient pattern whose strength depends on the magnitude of the initial signal derivatives at small time. These transients travel at velocity c_0 and constitute the precursory front of the wave. They oscillate more and

more rapidly with distance, until the envelope approximation begins to break down as the condition $\Lambda x \ll \omega_m$ is no longer fulfilled. Their maximum amplitude decays exponentially in time with time constant τ , but only as a power of $x^{-1/2}$ with distance, in contrast to the delayed part of the response, which is exponentially damped with distance. The precursors basically arise from the free decay of the Lorentz oscillator response. To illustrate these

properties, we consider a few special cases.

The response to a step perturbation, already dealt with in the preceding paragraph by a direct method, is, in principle, not given by Eq. (66) since a step input is not even differentiable once at the origin. However, the integral in Eq. (47) can also be evaluated asymptotically by the method leading to Eq. (66). The result of this evaluation, which gives

$$A(t, x) = e^{-s_0 t'} J_0(2\sqrt{\Lambda x t'}) + s_0 e^{-s_0 t'} \int_0^{t'} \frac{d}{du} e^{s_0 u} \Big|_{u=t'-t''} J_0(2\sqrt{\Lambda x t''}) dt''$$

$$= e^{-s_0 t'} \sum_{n=0}^{\infty} \frac{d^n}{du^n} e^{s_0 u} \Big|_{u=0} \left(\frac{t'}{\Lambda x} \right)^{n/2} J_n(2\sqrt{\Lambda x t'}), \quad (67)$$

has the same form as the general expression (66) and is nothing but the expansion (52). The leading term for small t' and large Λx is $J_0(2\sqrt{\Lambda x t'})$. It represents a precursor with a characteristic oscillating pattern which has been called a "0 π " pulse by Crisp.³⁵ This precursor, which corresponds to a step impulse with a discontinuity at the origin, does not decay with x . We shall call such a behavior a resonant precursor of zeroth order.

We note that the response to a Dirac impulse obtained in Sec. IV A and expressed by Eq. (46) also displays the same general form of Eq. (66). The oscillating part of the response in Eq. (46) (which in this case can hardly be called a precursor *since it follows the signal*) grows as $x^{1/2}$. It may be said to arise from a discontinuity of order -1 and to lead to an n th order precursor with $n = -1$.

Thus, quite generally, the n th-order precursor corresponds to a discontinuity of the n th derivative of the initial signal and behaves as $(t'/\Lambda x)^{n/2} J_n(2\sqrt{\Lambda x t'})$. The property of n th-order precursors to decay with the peculiar $x^{-n/2}$ dependence has been checked by direct computer simulation on Eq. (39) and is shown in Fig. 7. It must be noted that the decay with distance of the n th-order precursor plotted in Fig. 7 goes as $x^{-n/2-1/4}$. The extra $x^{-1/4}$ power comes from the asymptotic form for large arguments of the Bessel functions expressed by Eq. (56), as the small local-time part was not accurately resolved at large x by the computer calculation.

The physical origin of precursors can be viewed from two different standpoints. From the first point of view, they may be seen as a beat pattern which develops during the propagation of frequency components of the pulse lying below and above the absorption frequency. This interpretation stems directly from the derivation that we have just given. The observation that the precursors are composed of high- and low-frequency components makes quite understandable the fact that they travel through the resonant medium with low attenuation and with velocity c_0 .

The second point of view gives more insight into their physical nature. It is based on the well-known correspondence between the Lorentz oscillators, considered as two-level systems, and an assembly of spins $S = 1/2$.^{34,72} This correspondence enables us to draw on the various concepts

introduced in ESR or NMR spectroscopy and on the panoply of solutions of the Bloch equations.⁷³ We consider a given spin at x , at rest before the arrival of the traveling wave, i.e., aligned on the quantization axis carrying the equivalent magnetic field. The wave acts as a transverse excitation field and causes a nutation of the spin. The nutation angle is small since we only consider the linear response of the system. The nutation is accompanied by a Larmor precession at frequency ω_m . The Bessel-function response expressed by Eq. (66) results in the interplay between the incoming field and the induction resulting from the spin motion. The spins respond without delay to the suddenly varying incoming field: they act as quantum-mechanical tops endowed with zero transverse moment of inertia. If the dominant frequencies in the sudden excitation are high compared to ω_m , the Larmor precession will not be a significant part of the

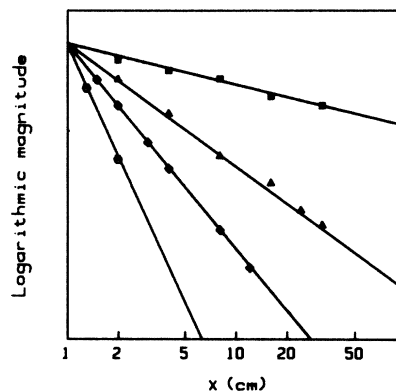


FIG. 7. Precursor magnitude as a function of distance on a log-log plot. The magnitudes are normalized at $x = 1$ cm, $\Delta\omega = 0$. The solid lines have slopes of 0.25, 0.75, 1.25, and 2.25, as required by the asymptotic dependence of $J_n(\sqrt{x})$ at large x . The symbols come from computer simulations: squares correspond to a step input ($\tau_H = 4 \mu s$) with $\lambda = 3.5 \times 10^{-6}$, $\tau = 10 \mu s$; triangles to one exponential convolution with $\tau_R = 8.5 \mu s$ [see Eq. (86)] with $\lambda = 3.5 \times 10^{-6}$, $\tau = 10 \mu s$; diamonds and hexagons to two and four exponential convolutions, respectively, with $\lambda = 10^{-5}$ and $\tau = 5 \mu s$.

precursory response. In all cases, the early spin response, and hence the precursors in the propagating wave, die off in a time of the order of the lifetime τ . In NMR terminology, τ is the transverse spin relaxation time, usually noted T_2 . If τ is long with respect to the propagating pulse duration τ_p , the energy lost to the medium is small because it is, for the most part, reemitted coherently in the traveling wave.

To make this point even clearer and to extend this description to high frequencies, let us retrace Sommerfeld's original derivation of the existence of precursors.^{10,46} The starting point is provided by Eq. (2), which we rewrite in the retarded frame at x as

$$\rho(t, x) = \int_{-\infty}^{+\infty} \rho(\omega) e^{-i\omega t' + iKx} \frac{d\omega}{2\pi}. \quad (68)$$

In the optical case considered by Sommerfeld, the wave vector is given by the Lorenz-Lorentz dispersion formula:

$$k = K + \frac{\omega}{c} = \frac{\omega}{c} \left[1 - \frac{\lambda_{LL}}{\omega^2 - \omega_m^2 + 2i\omega\tau} \right]^{1/2}. \quad (69)$$

The frequency dependence of the coupling constant λ_{LL} differs from that of the quantity λ used in this work because the form of the coupling terms in Eqs. (5) and (6) is not that relevant to the interaction of electric dipoles with the electromagnetic field. Accordingly, the high-frequency behavior of the two models will be different.

We borrow from Sommerfeld the argumentation according to which the small time response is linked to high frequencies and expand Eq. (69) to first order in ω_m/ω :

$$\begin{aligned} K &= \frac{\lambda_{LL}\omega}{2c} \left/ (\omega^2 - \omega_m^2 + 2i\omega\tau) \right. \\ &= \frac{\lambda'_{LL}}{2c} \left/ (\omega - \omega_m + i/\tau') \right. . \end{aligned} \quad (70)$$

We have redefined λ_{LL} and τ in such a way as to include a slow ω dependence by letting

$$\lambda'_{LL} = \frac{\omega}{\omega + \omega_m} \lambda_{LL}, \quad (71)$$

$$\tau' = \frac{\omega + \omega_m}{2\omega} \tau. \quad (72)$$

In the high-frequency limit, we shall have $\lambda'_{LL} = \lambda_{LL}$ and $\tau' = \tau/2$, while close to ω_m the coupling constant and the inverse lifetime are reduced by a factor 2. With $\Lambda' = \lambda'_{LL}/2c$ and using Eqs. (70)–(72), expression (68) for the signal at location x and local time t' becomes

$$\rho(t, x) = \int_{-\infty}^{+\infty} \rho(\omega) \exp \left[-i\omega t' + i \frac{\Lambda' x}{\omega - \omega_m + i/\tau'} \right] \frac{d\omega}{2\pi}. \quad (73)$$

As in Sec. III, we shift frequencies by letting $\omega' = \omega - \omega_m + i/\tau'$, and transform $\rho(\omega)$ according to the prescriptions of the envelope approximation. In other words, we transform to the spin-rotating frame.⁷³ The initial signal in the frequency domain corresponding to a truncated sine wave $\rho(t) = U_+(t) \sin(\omega_0 t)$ is

$$\rho(\omega) = 1/(\omega^2 - \omega_0^2). \quad (74)$$

We note that this initial signal is continuous at $x=0, t=0$ and that its first derivative shows a discontinuity. In our classification, it will give rise to a precursor of first order. The outcome of the envelope approximation is expressed by

$$\rho(t, x) = \text{Re} \left\{ \frac{1}{2} \exp \left[- \left[i\omega_m + \frac{1}{\tau'} \right] t' \right] \int_{-\infty}^{+\infty} \frac{e^{-i\omega' t' + i\Lambda' x/\omega'}}{\omega' - \omega_0 + \omega_m - i/\tau'} \frac{d\omega'}{2\pi} \right\}. \quad (75)$$

We can expand the denominator in the integrand in powers of $(\omega_0 - \omega_m - i/\tau')/\omega'$ (forgetting about the ω dependence of Λ' and τ') and integrate term by term to obtain, using Eq. (48),

$$\begin{aligned} \rho(t, x) &= \text{Re} \left\{ \frac{1}{2} \exp \left[- \left[i\omega_m + \frac{1}{\tau'} \right] t' \right] \int_{-\infty}^{+\infty} \frac{e^{-i\omega' t' + i\Lambda' x/\omega'}}{\omega'} \frac{d\omega'}{2\pi} + O_2 \right\} \\ &= \text{Re} \left\{ \frac{1}{2} \exp \left[- \left[i\omega_m + \frac{1}{\tau'} \right] t' \right] \left[\sum_{n=0}^{\infty} \left[s_0 \left(\frac{t'}{\Lambda' x} \right)^{1/2} \right]^{n/2} J_n(2\sqrt{\Lambda' x t'}) \right] \right\}. \end{aligned} \quad (76)$$

We recover our direct result⁵² with an important proviso about the ω dependence of Λ' and τ' . The dominant term of this expansion does reproduce, as expected, Sommerfeld's result in the limit $\omega_m \rightarrow 0$. The dependence on τ' which goes as $\exp(-2t'/\tau')$ has been derived by Brillouin.²⁸ Thus apart from factors of 2 in the coupling constant and the relaxation rate arising from Eqs. (71) and (72) and from the dependence on the Larmor precession frequency, the expressions for the precursor of first order

and Sommerfeld's are identical. The physical origin is the same in both cases and stems from the transient response of the spins in interaction with the propagating wave. At very high frequency, the motion of the rotating frame at the Larmor frequency is imperceptible. At frequencies close to ω_m , the perturbing field is stationary in the rotating frame and leads to the same response of the spins. We therefore reach the conclusion⁴⁶ that Sommerfeld's precursors constitute the high-frequency match to the phe-

nomena described by Eq. (66).

We have not identified Brillouin's low-frequency precursor on the time-domain expression (66), although a low-frequency transient response is visible in Fig. 5. This precursor, as well as that of Briman and Frankel,^{14,15} is a weaker feature which is masked by the stronger parts of the response. Besides, as noted by Crisp,³⁵ the envelope approximation fails by its very construction to describe accurately the low-frequency components of the signal, i.e., those whose contributions to the envelope lay in the vicinity of $\pm\omega_0$ and strongly overlap the carrier wave. We have shown how the high-frequency components could be recovered exactly at the price of the introduction of a weak frequency dependence in parameters Λ and τ . Such a trick loses its usefulness as ω goes to zero because this frequency correction, given by Eqs. (71) and (72), becomes large.

As the optical thickness Λx of the medium increases, the dominant frequency of the precursors $\Lambda x/2\pi$ also increases. Their ultimate fate depends on the attenuation mechanisms at high frequency. In superfluid $^3\text{He-B}$, they eventually run into the pair-breaking regime⁵⁰ at frequencies such that $\hbar\omega > 2\Delta$, in which they are quickly annihilated.

E. Signals with no marked front: Gaussian pulses

At this point we have fulfilled our goal to split the solution of coupled equations (5) and (6) into a transient part,

$$A(t, x) = \left[1 - \frac{2[t' - t_0 + \Lambda x / (i\Delta\omega + 1/\tau)^2]}{\tau_p^2 (i\Delta\omega + 1/\tau)} \right] \exp \left[-\frac{1}{\tau_p^2} \left(t' - t_0 + \frac{\Lambda x}{(i\Delta\omega + 1/\tau)^2} \right)^2 - \frac{\Lambda x}{i\Delta\omega + 1/\tau} \right]. \quad (77)$$

This expression will describe the propagation of a Gaussian pulse without distortion when a number of conditions are fulfilled. Let us study these conditions close to resonance for simplicity. Firstly, the asymptotic evaluation requires that Λx be large with respect to $1/\tau$. Secondly, the amplitude of the initial transient is very small if t_0 , the time at which the initial envelope reaches its maximum value, is much longer than τ_p , the width of the pulse. The fostered precursors are also very small with respect to the signal as long as $\exp(-\alpha x)$ is larger than $\exp(-t_0^2/\tau_p^2)$. Replacing the attenuation coefficient α by its on-resonance value, we obtain a third condition:

$$\Lambda x < \frac{t_0^2}{\tau_p^2}. \quad (79)$$

Lastly, Eq. (59) yields a pulse whose shape does not change during propagation only if the term in $dA(t)/dt$ is small with respect to the undistorted contribution. This condition implies the following inequality:

$$\Lambda x < \frac{\tau_p^2}{2\tau^3}. \quad (80)$$

Thus, a Gaussian pulse propagates unaltered in shape over distances set by Eq. (79) or by Eq. (80) with a faster-than-light or negative group velocity if the following inequali-

ties are satisfied:

$$t_0 \gg \tau_p \gg \tau \gg 1/\Lambda x. \quad (81)$$

Applying the general result of the asymptotic evaluation of slowly varying envelopes expressed by Eq. (59), we find

ties are satisfied:

$$t_0 \gg \tau_p \gg \tau \gg 1/\Lambda x. \quad (81)$$

The modulus of the pulse envelope is then given by

$$A(t, x) = \exp \left[-\alpha x + \frac{\alpha_g^2 x^2}{\omega_0^2 \tau_p^2} \right] \times \exp \left[-\left(t - \frac{x}{c_g} - t_0 \right)^2 / \tau_p^2 \right]. \quad (82)$$

This expression, which is the product of a Gaussian pulse of width τ_p traveling at velocity c_g and an exponential attenuation factor, is identical to that obtained by Macke²³ using a different time-domain analysis. The set of conditions that we have derived above for the validity of Eq. (82) also ensures that causality is preserved in all cases, that is, the maximum negative delay on resonance, $-\Lambda x \tau^2$, is always much less in magnitude than t_0 . The attenuation factor in Eq. (82) also calls for some comments. The damping of the propagating pulse does not follow Beer's law, as the exponent is not linear in x . The quadratic term is due to the imaginary part of the complex group velocity given by Eq. (64) and describes pulse reshaping. We note that, depending on the sign of the shift from resonance $\Delta\omega$, we may have either an attenua-

tion or an amplification of the wave, and that this effect increases with distance as x . At first glance, this may appear as an unphysical result. However, the term in $(\alpha_g x / \omega_0 \tau_P)^2$ is always a small correction owing to Eq. (80), which expresses the condition that the pulse propagates undistorted. We meet here a specific example of the role of the imaginary part of the signal velocity in pulse reshaping.

If we relax condition (80), the pulse will suffer distortions described asymptotically by our general result (59). In spite of these distortions, it may still be said that the distorted pulse is traveling at the complex group velocity because the general form of Eq. (59) allows an unambiguous definition of the "delayed" signal. Over a short length span, say between x and $x + dx$, the "delayed" signal suffers little more distortion and does travel with velocity c_g .

In addition, the exact shape of the pulse is not necessarily recorded in actual experiments. For instance, if the propagation velocity is defined, as is often the case^{64,74,75} as the velocity of the crest of the pulse envelope, the influence of the term in dA/dt in Eq. (59) is reduced and the velocity measured according to such a criterion remains closer to the classical group velocity over a wider range of situations than suggested by Eqs. (79)–(81). Such a result can, of course, be expected to hold on general grounds since the envelope is very slowly varying about the crest.

To provide both a check of our analysis and an illustration of the propagation of pulses of arbitrary shape but without a well marked front, we have made a computer simulation in a physical situation corresponding to ³He-B with the following parameters: $\lambda = 10^{-3}$, $\tau = 1 \mu\text{s}$, $\omega_0/2\pi = 45 \text{ MHz}$, and $c_0 = 310 \text{ m/s}$. The initial pulse without a sharp front is constructed according to a prescription which will be justified in the next section. It involves an eightfold convolution of a rectangular rf pulse of $4 \mu\text{s}$ duration with a first-order response function with

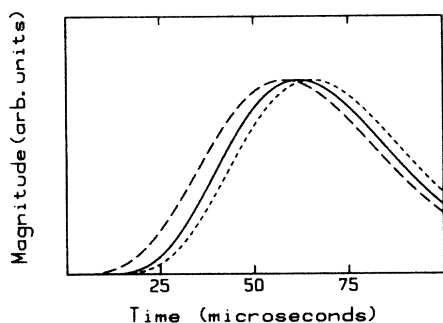


FIG. 8. Normalized pulse shapes at $x = 0.025 \text{ cm}$ for an initial envelope with no marked front. The initial envelope is generated by filtering a rectangular input with $\tau_{\text{eff}} = 4 \mu\text{s}$ through an eightfold exponential convolution with $\tau_R = 8.5 \mu\text{s}$. The medium parameters are $\lambda = 10^{-3}$, $\tau = 1 \mu\text{s}$, $c_0 = 310 \text{ m/s}$, corresponding to the squashing mode in ³He-B at 13.5 bars in the vicinity of T_c . The solid line is obtained far from resonance ($\Delta\omega = 10^8 \text{ rad/s}$), and the corresponding attenuation is less than 0.1 cm^{-1} . The short-dashed line is for $\Delta\omega = 2 \times 10^6 \text{ rad/s}$, $\alpha = 255 \text{ cm}^{-1}$; the long-dashed line for $\Delta\omega = 1 \times 10^6 \text{ rad/s}$, $\alpha = 630 \text{ cm}^{-1}$. The long-dashed signal has propagated with faster than c_0 velocity and has experienced little distortion.

characteristic time $\tau_R = 8.5 \mu\text{s}$. The derivatives of the resulting signal are thus continuous at the origin of time up to the seventh order. The corresponding precursor decays with distance as x^{-4} . Over a path length of $x = 0.025 \text{ cm}$, the main part of the signal largely overwhelms the precursor, which can therefore be discarded. The signal at location x is computed from the full expression (33) for the envelope and is shown in retarded and advanced situations in Fig. 8. It is said to have arrived, according to Brillouin's definition,¹¹ when its amplitude has reached a certain fraction, e.g., $\frac{1}{3}$, of its peak amplitude. The results of this simulation are shown in Fig. 9, where they can be compared to the classical group velocity. The signal is seen to speed up again in the anomalous dispersion region; its velocity tracks the classical group velocity to a reasonable accuracy, certainly much better than it follows Brillouin's result, which never exceeds c_0 , not to mention Baerwald's velocity expressed by Eq. (54), which, as we have already mentioned, stems from a different definition of the signal arrival time.

We shall present in the next section our experimental results on acoustic wave pulses with a well-defined beginning, which, when the "delayed" signal is identifiable, lead to the same behavior as that illustrated in Fig. 8. Other experiments in the optical and microwave domains, mentioned in the Introduction, exhibit the same pattern. It seems difficult to escape the conclusion contained in our general result (59) that pulses with no marked front do propagate with a signal velocity which is identical in a first approximation to the classical group velocity both inside and outside of the anomalous dispersion region. When a well-defined wave front is present, precursors come in, but a part of the response can still be separated

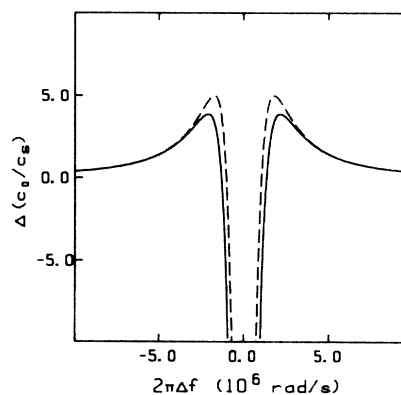


FIG. 9. Shift in signal (solid line) and group (dashed line) velocities vs departure from resonance for input envelopes with no marked front. The signal velocity is obtained numerically from the pulse envelopes shown in Fig. 8 from the time at which the signal reaches $\frac{1}{3}$ of its peak value. Both velocities are seen to track reasonably well even in the anomalous dispersion region where they become larger than c_0 , infinite, or even negative. The results shown above hold for Δx large enough for Eq. (59) to be asymptotically valid, but small enough for the precursors, suppressed up to order 7, to remain smaller than the "delayed" signal. At large distance, precursors take over and c_s falls back to c_0 .

that travels with the classical group velocity as long as causality is preserved.

V. TRANSMISSION OF SOUND IN $^3\text{He-B}$

In this section we describe first the experimental setup which led to the results shown in Fig. 1 as well as to more detailed studies of the real squashing and squashing modes which are directly relevant to the topic of this paper. We then give a characteristic example of each situation.

The experiments are carried out in a copper nuclear demagnetization cryostat^{76,77} capable of maintaining temperatures below 1 mK for times of the order of a week. The primary thermometry is provided by a Pt NMR spectrometer. It is believed⁷⁸ that the absolute temperature is known to be about 5%. Temperatures relative to the superfluid transition temperature T_c , namely T/T_c ratios, are known to an accuracy of the order of 1%, except possibly at the lowest temperatures ($T < 0.5$ mK). The knowledge of the temperature is important in these mode-crossing experiments because the sound transducers operate at constant frequency and the mode resonance is temperature dependent: the sound and pair-vibration modes are made to cross by sweeping the temperature. An example of such a temperature sweep is shown in Fig. 1. The mode frequency is related to the temperature by

$$\hbar\omega = a \Delta(T), \quad (83)$$

where $\Delta(T)$ is the gap parameter.^{47,49} The weak-coupling theoretical values of a are $(\frac{8}{5})^{1/2}$ or $(\frac{12}{5})^{1/2}$ for the real squashing and squashing mode, respectively. The strong-coupling Fermi-liquid, and higher-orbital-wave corrections are still rather uncertain, but are found experimentally to be, at most, of the order of 10–20%.^{52,78,79} These corrections are not significant in the present context and shall not be taken into account. The gap function $\Delta(T)$ is given by the BCS theory.⁸⁰

Differential frequency shifts are obtained from temperature drifts by the following relation:

$$\delta\omega = 1.764a (k_B T_c / \hbar) \frac{d[\Delta(T)/\Delta(0)]}{dT} \delta T. \quad (84)$$

The quantity k_B/\hbar is equal to 20.8 MHz/mK and $1.764k_B T_c$ gives the zero-temperature BCS gap $\Delta(0)$. The quantity $\Delta(T)/\Delta(0)$ is, in the BCS theory, a universal function of T/T_c .⁸⁰

The sonic cell is made up of two X -cut quartz transducers separated by a 4.00-mm quartz spacer. The spacer is polished to optical flatness and parallelism. The transducers are mounted using a technique of semiadherence, which is common practice in optical lens assembly. The lack of parallelism between the transducers (of diameter 4.5 mm) is believed to be less than 0.2 μm . The quartz crystals have a fundamental frequency of 14.7 MHz (matched to 150 Hz). They can be usefully operated at odd harmonics up to the thirteenth.

The sonic transducers, located in the very-low-temperature experimental chamber, which is filled with superfluid ^3He , are connected to the room-temperature rf transmitter and preamplifier by low-loss 50- Ω transmis-

sion lines. These transmission lines preserve the shape of the rf signals. The initial signal from the electronic transmitter is a rf toneburst of rectangular envelope and of duration τ_{rf} . The Laplace transform of such a signal is

$$A_{\text{rf}}(s) = [1 - \exp(-\tau_{\text{rf}}s)]/s. \quad (85)$$

When this electrical signal, which possesses a true beginning and end, is transformed within the piezoelectric crystal into a mechanical signal, it experiences a convolution with the response function $H(s)$ of the transducer. $H(s)$ involves the exponential ringing time constant τ_R :

$$H(s) = A_{\text{out}}/A_{\text{in}} = 1/(s + 1/\tau_R). \quad (86)$$

We note here that a second-order electromechanical system yields a response function for the envelopes which is first order only. The value of the ringing time constant τ_R is essentially governed by the loading of the quartz crystal by the surrounding liquid. The acoustic impedance offered by superfluid $^3\text{He-B}$ has been studied in Ref. 57. From Eqs. (85) and (86) we find that the shape of the envelope emitted into the liquid is given by

$$A(s) = H(s)A_{\text{rf}}(s). \quad (87)$$

At the receiving end, this envelope has traveled through the liquid according to Eq. (33). It experiences one more convolution with the response function (86) in the receiving crystal in such a way that, if the liquid were a perfectly nondispersive, transparent medium, the received envelope would be represented by

$$A(s) = H^2(s)A_{\text{rf}}(s). \quad (88)$$

The rf signal is then processed in a way which can be traced on the block diagram of the electronics given in Fig. 10. It is first amplified in a broad band preamplifier and heterodyned to an intermediate frequency of 35 MHz. The following amplifying stage has a bandwidth of 5 MHz about the intermediate frequency. The amplified signal is demodulated by two mixers driven with reference signals at 35 MHz in exact quadrature. We thus obtain the two components of the complex envelope which are fed into two transient signal recorders with a time resolution of 50 ns. These recorders are interfaced to a desk computer which controls the whole experiment and computes the amplitude and the phase of the signal. The computer subtracts vectorially a baseline which contains a record of the spurious signals of electrical and acoustic origin, in order to lower the detection threshold of useful signals. It performs checks on the overall amplitude of the received signal and actuates an attenuator which keeps this amplitude within the linear dynamical range of the receiver. The data processing also includes a least-squares parabolic smoothing on 13 adjacent points.⁸¹ This digital-filtering step fixes the detection bandwidth of the receiver and limits the maximum signal rise time to about 0.5 μs . The bandwidth limitation due to the crystal response function (86) can be, within limits, removed by a deconvolution process. As mentioned in Sec. III, the above sequence of signal-processing operations tailors the received signal to fit very neatly into the framework of the slowly varying envelope approximation.

We present in Fig. 11 the observed signal amplitudes and phases obtained by sweeping the temperature through the real squashing mode in $^3\text{He-B}$ at a pressure of 1.2 bars and a frequency of 45 MHz. The temperature at which the real squashing mode crosses the zero-sound mode in these conditions is $0.625 T_c$, with $T_c = 1.26$ mK. The top curve in Fig. 11 relates to the signal far from resonance, plotted in arbitrary units as a function of time in the local reference frame. Its amplitude and phase are described by Eq. (88). The ringing time τ_R is adjusted starting from the theoretical value to fit the received signal. This theoretical value is governed⁵⁷ by the real part of the acoustic impedance which, far from the mode-crossing region, is $Z' = \rho c_0$ (ρ being the density):

$$\tau_R = \pi Z_Q / 2\omega_f Z' \quad (89)$$

The quantities $\omega_f/2\pi$ and Z_Q are the fundamental frequency and acoustic impedance of the quartz crystal.⁸² At 1.2 bars, Eq. (89) gives a time of $15.1 \mu\text{s}$. Adding the intrinsic damping of the crystal measured *in vacuo* brings this value down to $10 \mu\text{s}$. The fitted value is $8.5 \mu\text{s}$. The difference between the two last values is mainly due to the fact that, for short excitation times, $\tau_{rf} < \tau_R$, the ringing decay is not quite exponential. In spite of this slight im-

perfection, the received signal far from resonance is well described by the double-exponential convolution of a rectangular pulse, as shown in Fig. 11.

The bottom curve in Fig. 11 is obtained close to resonance. Its amplitude has been magnified by a factor 12.9 with respect to the top curve. This signal displays the characteristic wiggles of precursors. Its phase changes by π at each extinction point of the envelope, indicating a sign reversal. The extinction points become more and more distant from one another as time t' evolves, in

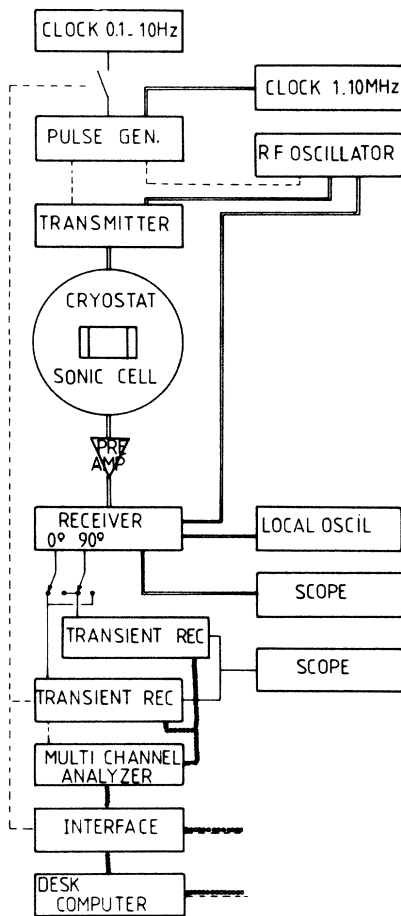


FIG. 10. Block diagram of the electronics of the sound-propagation experiment.

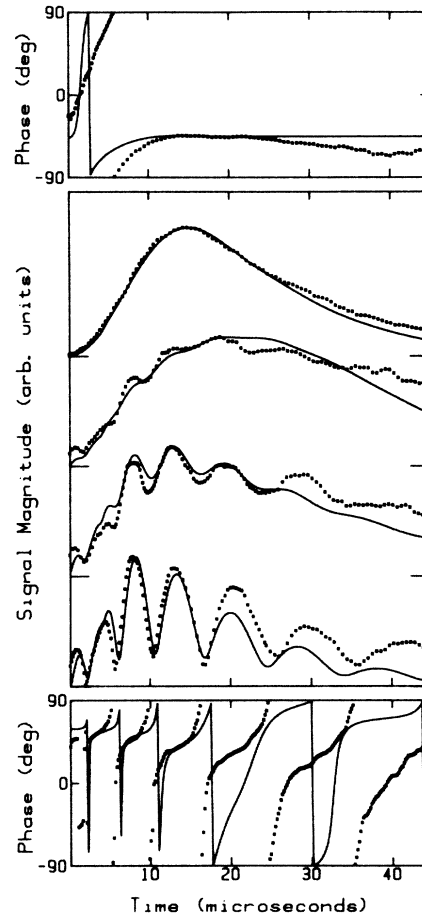


FIG. 11. The experimental (dots) and calculated (solid line) received signal amplitude and phase as functions of time at various temperatures in the vicinity of the real squashing mode in $^3\text{He-B}$ at 1.2 bars, 45 MHz. The on-resonance temperature is $0.625 T_c$ ($T_c \sim 1.26$ mK). The top and bottom curves represent the phase variation and relate to the top and bottom amplitude curves, respectively. The former corresponds to a situation far from resonance ($\Delta\omega = 9.4 \times 10^5$ rad/s). The latter corresponds to a situation close to resonance ($\Delta\omega = 6.4 \times 10^4$ rad/s), and has been magnified by a factor 13 with respect to the top curve. The two other amplitude curves correspond, respectively, to $\Delta\omega = 2.4 \times 10^5$ and 4.3×10^5 rad/s and have been magnified by 8.8 and 4.8, respectively. The solid lines are signals computed from Eq. (33) with $\lambda = 3.7 \times 10^{-6}$, $\tau = 10.7 \mu\text{s}$, $c_0 = 202$ m/s, corresponding to a rectangular initial envelope with $t_{rf} = 4 \mu\text{s}$, convoluted exponentially once with $\tau_R = 8.5 \mu\text{s}$, as explained in the text.

agreement with the square-root dependence of the Bessel-function argument in Eq. (66). Signals off resonance are also shown in Fig. 11. The solid curves are obtained from Eqs. (33), (34), and (20) with $\lambda=3.7\times 10^{-6}$ and $\tau=10.7\ \mu\text{s}$, using a fast-Fourier-transform algorithm. The agreement between calculations and observations is quite satisfactory. It shows how a dephasing factor coming from a shift from the resonance frequency gradually erases the precursors and restores the initial shape of the signal.

Although the discussion of the preceding section leaves no room for ambiguity, we emphasize here that the wiggling pattern of precursors is a linear effect. In particular, it is *a priori* not related to the pulse breakup at high power level observed by Polturak *et al.*⁸³ which is believed to be a nonlinear effect.⁸⁴ In the course of the experiment, we have performed linearity checks by varying the excitation level by a factor 2, i.e., power level by a factor 4. The maximum total energy in the sound pulse per unit area used in these experiments amounts to 10^{-4} erg/cm² for $\tau_{\text{rf}}=4\ \mu\text{s}$, that is, with a sound velocity $c_0=233$ m/s a maximum energy density of the order of 10^{-3} erg/cm³.

Complying with usual practice, we have used the following operational definitions of the signal velocity and attenuation coefficient. The signal arrival time is defined by the time at which the signal reaches $\frac{1}{3}$ of its maximum amplitude; it is thus independent of the detector sensitivity, which is assumed to be always adequate, but it will be strongly affected by the change in shape of the signal. The amplitude attenuation coefficient is computed from the ratio of the observed peak amplitude to a reference

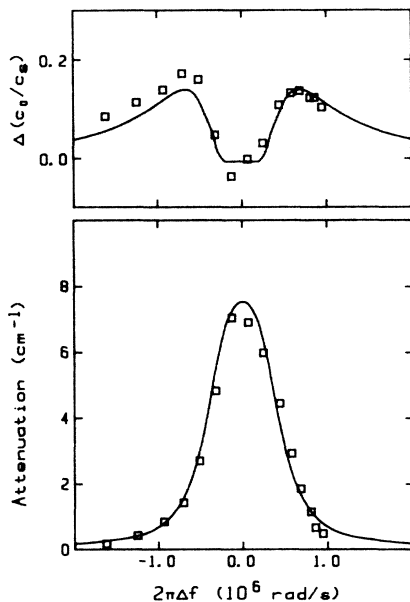


FIG. 12. Measured (squares) and calculated (solid line) attenuation coefficient and inverse signal velocity change as functions of the departure from resonance. The cw peak attenuation would be $80\ \text{cm}^{-1}$ for the case studied here. The delayed signal velocity, as computed from Eq. (63), is given in Fig. 6. It is clear both from the signal shapes in Fig. 11 and from the curves shown above that the sonic response is dominated by the precursors in the anomalous dispersion region.

level defined as the limit in the case where no damping is present. This reference amplitude is an instrumental constant which depends on frequency. It has been determined by two separate experiments. First, in ^3He in the normal (i.e., nonsuperfluid) state, zero-sound damping decreases with temperature as T^2 and is independent of frequency, at least as long as quantum effects can be neglected. A fit to this quadratic temperature dependence yields the zero-attenuation level. The second method takes advantage of the fact that damping in the *B* phase becomes very small at temperatures very low with respect to T_c and frequencies far from any pair-vibration modes and from the pair-breaking region. These two methods agree to better than $0.1\ \text{cm}^{-1}$.

We have plotted the attenuation coefficient α and the inverse signal velocity $\delta(c_0/c_s)$ variation obtained from the real and computer-simulated signals in Fig. 12. This figure calls for several comments. The signal velocity is seen to follow the general behavior already met in Figs. 6 and 9, that is, a slowing down of the signal which reverses itself in the immediate vicinity of the resonance and becomes close to the unperturbed sound velocity. This effect here is due to precursor takeover and not to the re-entrance of c_s . It gives rise to the flat portion of the curve about $\Delta\omega=0$. The apparent attenuation peaks at about $7.5\ \text{cm}^{-1}$ with a full width at half maximum (FWHM) of $2/\tau=0.874\times 10^6$ rad/s. The cw attenuation at maximum, as computed from Eq. (40), is equal to $78.3\ \text{cm}^{-1}$ with a FWHM of $2/\tau=0.187\times 10^6$ rad/s. The precursors reach their peak about 245 dB above the level of the continuous wave: the medium is quite transparent to pulses of duration τ_{rf} of the order of τ . Both λ and τ are seriously in error if due care is not given to this transparency effect in the analysis of sonic data.^{51,56}

Figures 11 and 12 show without ambiguity that Eq. (33) yields a quite accurate representation of the observed sound signals in the vicinity of the real squashing mode. The various properties of signals and first-order precursors that we have derived from Eq. (33) in Sec. IV are found in the observed signals in a better than qualitative manner: the precursor extinction points are given by the zeroes of $J_1(2\sqrt{\Lambda x t'})$, and its amplitude is well approximated by

$$(A_0/\tau)(\tau t'/\alpha_m x)^{1/2} J_1(2\sqrt{\Lambda x t'}) \exp(-t'/\tau).$$

Another illustration of precursors is provided by the beautiful subpicosecond detection experiment in the optical domain of Rothenberg *et al.*⁴⁵ This experiment yields pulse envelopes for the electromagnetic field which are strikingly similar to those of Fig. 11. The experimental evidence coming from both works, Refs. 6 and 45, leaves actually no room for doubt.

We now turn to another mode-crossing situation, that provided by the squashing mode, which strongly repels the zero-sound mode. At temperatures below $0.8T_c$ or so, the lifetime has become large enough for the strong-repulsion regime to prevail (see Fig. 4). A striking feature of this regime resides in the existence of very long group delays. Group velocities smaller than $c_0/10$ have been recorded in $^3\text{He-B}$ at 3.5 bars and 75 MHz, as shown in Fig. 13. This figure illustrates a situation in which

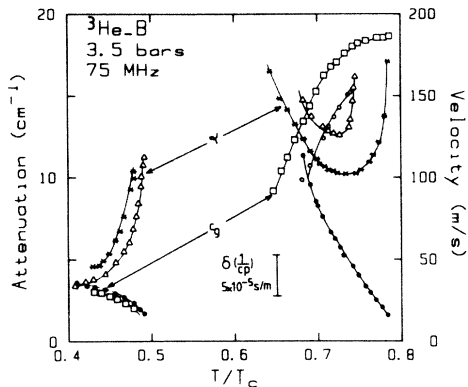


FIG. 13. Measured attenuation coefficient, group velocity, and inverse phase velocity change vs temperature in the vicinity of the squashing mode at 3.5 bars and 75 MHz, for two values of magnetic fields applied along the direction of sound propagation (*, attenuation; □, group velocity; ● $\delta(1/c_p)$ at $H_0=0$ G; △, attenuation; ○, group velocity at $H_0=1000$ G). This figure shows a regime of very slow group velocity combined with low attenuation and should be compared qualitatively to the computed group velocities in Fig. 4.

strongly dispersive effects coexist with small attenuation. This situation, which is quite similar to that of polaritons or exciton-photon—propagating bound states,⁸⁵ lies outside the scope of this study. In particular, boundary conditions play an important role, as shown by acoustic impedance studies.⁵⁷ Let us, as a side remark, mention that precursors were seen neither on the detected output nor on a wideband oscilloscope connected at the preamplifier output: their predicted frequency, as shown in Fig. 14 obtained by computer simulation, is quite high. Precursors in this strong-mode-repulsion case have been observed by Pleshko and Palócz³² in wave guides, but their existence in matter has still to be demonstrated.

VI. CONCLUSIONS

We have studied the propagation of pulses in a medium exhibiting a well-defined resonance weakly coupled to the propagating wave. In the case of Lorentzian line shapes and for a broad class of pulses with a bounded spectrum, or, in the case of strong mode repulsion and for pulses with a bounded but broad spectrum, the medium dispersion law can be represented by Eq. (1) and the pulse envelope at location x by the time-convolution integral (4) or the Fourier integral (33). These expressions are more useful than the exact solution (2) because they are amenable to precise computer simulations and to asymptotic analytical evaluations.

According to the results derived in Sec. IV, the propagation of pulses shows the following general features.

True signals possess a well-marked beginning, for instance, at $t=0$: this is the very condition by which causality may be defined. Such signals give rise to a causal response at any later time, i.e., they never propagate faster than c_0 . Their front is marked by the discontinuous occurrence of a nonzero derivative of rank n at

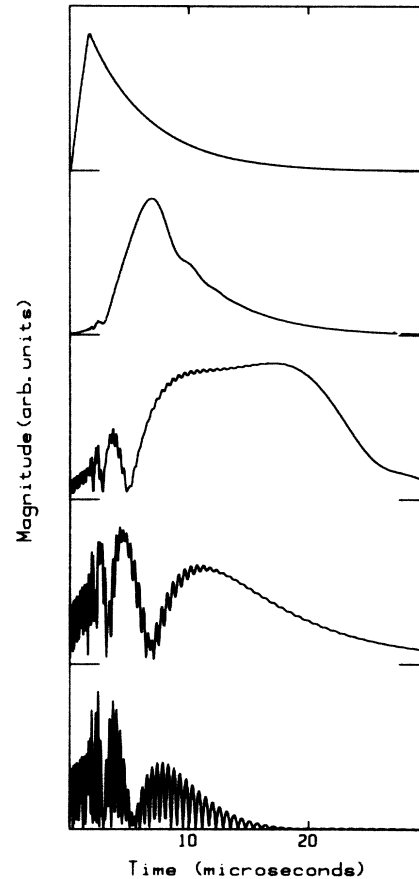


FIG. 14. Computed signal shapes as functions of time in the case of the squashing mode at 13.5 bars with $\lambda=10^{-2}$, $\tau=5$ μ s, $c_0=310$ m/s at a frequency of 45 MHz. The initial envelope is a rectangular pulse with $t_H=1.5$ μ s filtered by a single exponential convolution with $\tau_R=5$ μ s. In this computer simulation, the full dispersion curve has been used in Eq. (33). From top to bottom, the curves correspond to $\Delta\omega=50 \times 10^6$, 8×10^6 , 4×10^6 , 2.5×10^6 , and 0 rad/s, magnified by 1, 2.7, 34, 105, and 110, respectively. The sound flight path is 0.25 mm. It is seen that, even for such a small path, the precursor envelope oscillates quite rapidly. The slow modulation of the fast resonant precursors arises from interference between transients from the leading and falling edges of the input envelope.

$t=0$. Such discontinuities in time of the initial envelope generate transients. These transients travel at velocity c_0 and precede the rest of the signal. Generalizing a concept introduced by Sommerfeld and Brillouin, we call these transients precursors.

Precursors arise from the free response of the Lorentz oscillators. Their general expression (65) contains the prefactor $\exp(-i\omega_m t - t/\tau)$: they are modulated at the Larmor frequency ω_m and decay in time with the transverse relaxation time τ . For an n th-order discontinuity, the leading precursor develops a characteristic wiggling pattern going as $(t'/\Lambda x)^{n/2} J_n(2\sqrt{\Lambda x t'})$. They decay with distance not exponentially, but as $x^{-n/2-1/4}$ for their long-time part, or $x^{-n/2}$ at the maximum. Therefore, the purely transient response quickly overcomes the smoother

parts and makes up the truly elephantine⁹ feature of the received signal. The pseudofrequency of their envelope at fixed local time t' increases as Δx . When this pseudofrequency is much larger than ω_m , they become identical to Sommerfeld's well-known precursors. In the case studied here, where the Larmor modulation plays an important role, we call these features "resonant precursors"⁸⁶ in order to draw a distinction between them and Sommerfeld's high-frequency precursors and Brillouin's low-frequency precursors, although they all arise from the spin-transient response.

As the wave equations (5) and (6) are linear, solutions can be superposed and discontinuities in the signal elsewhere than at the wave front will display the same behavior as precursors.

Smooth portions of the initial envelope propagate differently according to whether they vary rapidly or not on a scale fixed by τ . Short pulses travel at velocity c_0 with little attenuation and give rise in their wake to a wiggling tail which is a "precursor" of order -1 . Signals which are not rapidly varying on this timescale are attenuated exponentially with distance and experience group delay and distortion as described by Eq. (59). When due allowance is made for their change in shape, they can be said to propagate with the classical group velocity throughout the anomalous dispersion region as long as causality is preserved. Such a shape alteration is always present when the signal is delayed, even far from the mode-crossing region. Insisting on no shape alteration to apply the concept of group velocity would restrict very narrowly its range of validity. In our view, severe pulse deformation does not prevent the group velocity, as defined by Eq. (59), from providing a valid description of the pulse motion from x to $x + dx$. A vivid illustration of the usefulness of the result (59) is provided by the propagation of signals with no marked front, such as Gaussian pulses. These signals, for which precursors are suppressed, can be seen to propagate with faster-than-light, or negative, velocities over a certain depth in the medium. Such group velocities should not be considered unphysical, but simply as the propagation velocity of a low-frequency (sine-wave) modulation on top of a high-frequency carrier wave. This modulation carries the same type of information as the phase of the carrier wave. In this formulation, the group velocity, including its imaginary component, always has a well-defined meaning.

Thus, our result (59) represents an extension of the group-velocity concept to distorted signals in the anomalous dispersion region of a Lorentz medium. One of the main consequences of this result, together with the realization of the true nature and importance of precursors, is to bring together various notions about the velocity of signals and recent experimental advances in resonant pulse propagation. These concepts have now been tested in practice and not just in theory.¹ Baerwald's approach has been shown to represent the time, given by Eq. (54), at which transients leave room to the long-lived part of the signal, if any. It also corresponds to the steady-state velocity of energy in the medium. This quantity is markedly different from the group velocity in the anomalous dispersion region. Brillouin's insightful formulation is

imprecise by nature since it is based on the shape of an integration path in the complex plane that can be deformed freely within large limits. In spite of this arbitrariness, it yields results, embodied in Eq. (65), which are not in gross conflict with the views presented here. In particular, it does contain the essential fact that, in the anomalous dispersion region, meaningful information propagates with near-maximum velocity. It can, however, not be said to provide more than a rough qualitative discussion of the phenomena involved in resonant pulse propagation.

We view received signals as being made up of several parts: a "delayed" signal which carries information on the original shape of the envelope and precursors generated by the various kinks in the original envelope. As the flight path increases, the "delayed" signal is attenuated exponentially while the precursors are damped with a much weaker length dependence and their pseudofrequency increases. The arrival time of the signal, defined by a given fraction of its peak amplitude, depends on the competition between these various parts, which, in turn, depends on the distance. Also, as the weight of high frequencies in the received signal spectrum grows with distance, the detector bandwidth becomes an important factor. The actual signal velocity, its shape, its information content, etc., result in the interplay of these different factors and are a matter of the particular circumstances of the experiment at hand. A few cases, close to experimental situations and showing the various aspects that we have just discussed, have been illustrated in Sec. V. It is also clear that one can meet other cases⁴² in which all constituents are completely entangled with one another because the front rise times are neither large nor small with respect to τ , or because the propagation length does not warrant the validity of the asymptotic evaluations. In these intermediate cases, our description is no longer useful. A full numerical solution, using Eq. (33), is then needed to obtain the shape of the propagated pulse.

A number of questions are still left open. Although our discussion seems to imply that a smooth wave packet always propagates with the classical group velocity, this result has been established only in the (slightly extended) case of a Lorentzian resonance line. From the work of other authors,^{9,12} the generalization seems warranted, but a proof encompassing all cases appears to be still lacking.

The results obtained in this paper are based on various approximations, such as the slowly varying envelope approximation and on asymptotic evaluations of integrals. No estimate of the errors have been given here, apart from a few comparisons with numerical computations. This problem is being tackled by Macke *et al.*⁸⁷ using a new operational approach.

The resonant medium has been considered here as homogeneous. Extension to the case of inhomogeneities on a microscopic scale has been treated in particular by Shiren¹⁸ and Crisp:³⁵ no qualitative changes are brought to the results. Large-scale inhomogeneities pose a completely different problem of their own,² a problem which might be relevant to a number of experimental situations where precursors should have been seen but were not.⁸³

Nonlinear effects^{84,88} have not been considered, although the slowly varying envelope approximation is, in

fact, designed to deal with these effects. It does lead⁸⁹ to interesting indications that, at least far from resonance, the signal velocity in the self-induced transparency case merges into the classical group velocity.

Also, the fresh but short insight which has been given to precursors is far from complete. This interesting phenomenon certainly deserves more experimental studies, particularly on their ultimate decay at large distance and high frequencies, and also in non-Lorentzian situations. Neither Brillouin's precursor, seen in an artificial delay line only,³² nor the excitonic precursor predicted by Frankel and Birman,¹⁵ have so far been identified in matter. We have also failed to identify them on computer simulations using reasonable input parameters mimicking the squashing mode in superfluid ³He-*B*, and conclude tentatively that, in the situations that we have studied, they form a very weak part of the transmitted signal. Further work on these open questions, for which both acoustical studies in ³He-*B* and ultrashort-pulse propagation in optical systems like that of Ref. 45 should prove to be quite valuable, is clearly desirable.

ACKNOWLEDGMENTS

We wish to acknowledge pleasant and fruitful discussions with B. Macke. This work has been supported in part by Direction de la Recherche et Etudes Techniques under Contract No. 79/567.

APPENDIX

The purpose of this appendix is to show that the slowly varying envelope approximation carried out as is conventionally done^{33,34} also leads to the approximate dispersion relation (1).

As a well-defined wave packet contains many periods of the carrier wave, we can replace the density fluctuation $\rho(t, x)$ by two slowly varying functions, the (real) amplitude $A(t, x)$ and the phase $\phi(t, x)$, by letting

$$\rho(t, x) = A(t, x) \cos \xi, \quad (\text{A1})$$

with $\xi = \cos[\omega_0(x/c_0 - t) + \phi]$.

The two functions A and ϕ describe the behavior of the components of ρ in phase and out of phase with $\omega_0(t - x/c_0)$. The pair-vibration amplitude can likewise be represented by

$$\delta(t, x) = D(t, x) \cos \zeta + E(t, x) \sin \zeta. \quad (\text{A2})$$

The conditions that the amplitude and phase of the signal are slowly varying functions of space and time are expressed by the following inequalities:

$$\left| \frac{\partial A}{\partial t} \right| \ll \omega_0 |A|, \quad \left| \frac{\partial A}{\partial x} \right| \ll \omega_0 |A| / c_0, \quad (\text{A3})$$

$$\left| \frac{\partial \phi}{\partial t} \right| \ll \omega_0, \quad \left| \frac{\partial \phi}{\partial x} \right| \ll \omega_0 / c_0.$$

Provided that the coupling constants and the damping terms are not abnormally large, the simplifications arising

from Eqs. (A3) lead to the following set of equations of wave motion:

$$\frac{\partial A}{\partial t} + c_0 \frac{\partial A}{\partial x} = -\frac{\omega_0}{2c_0^2} \gamma_0 E, \quad (\text{A4})$$

$$A \left[\frac{\partial \phi}{\partial t} + c_0 \frac{\partial \phi}{\partial x} \right] = -\frac{\omega_0}{2c_0^2} \gamma_0 D, \quad (\text{A5})$$

$$\frac{\partial D}{\partial t} = \left[\Delta \omega - \frac{\partial \phi}{\partial t} \right] - \frac{D}{\tau}, \quad (\text{A6})$$

$$\frac{\partial E}{\partial t} = - \left[\Delta \omega - \frac{\partial \phi}{\partial t} \right] D + \frac{\omega_0}{2c_0^2} \gamma_m A - \frac{E}{\tau}, \quad (\text{A7})$$

where

$$\Delta \omega = \left[\omega_0^2 \left(1 - \frac{c_m^2}{c_0^2} \right) - \omega_m^2 \right] / 2\omega_0.$$

These equations are the linearized form of the usual self-transparency equations.^{33,34} For this problem, they are particularly useful on resonance ($\Delta \omega = 0$) (Ref. 33) because ϕ and D remain identically zero. In the present situation, for which $\Delta \omega$ may be different from zero, the nonlinearities introduced by the polar representation constitute a drawback. Hence, we revert back to Cartesian coordinates for ρ , go to the rotating frame for E and D , and introduce, explicitly, the retarded local time $t' = t - x/c_0$:

$$X(t', x) = A(t', x) \cos \phi(t', x),$$

$$Y(t', x) = -A(t', x) \sin \phi(t', x),$$

$$U = E \cos \phi - D \sin \phi,$$

$$V = -E \sin \phi - D \cos \phi.$$

We obtain the following set of equations:

$$\frac{\partial X}{\partial x} \Big|_{t'} = -\frac{\omega_0}{2c_0^3} \gamma_0 U, \quad (\text{A8})$$

$$\frac{\partial Y}{\partial x} \Big|_{t'} = -\frac{\omega_0}{2c_0^3} \gamma_0 V, \quad (\text{A9})$$

$$\frac{\partial U}{\partial t'} \Big|_x = \Delta \omega V + \frac{\omega_0}{2c_0^2} X - \frac{U}{\tau}, \quad (\text{A10})$$

$$\frac{\partial V}{\partial t'} \Big|_x = -\Delta \omega U + \frac{\omega_0}{2c_0^2} Y - \frac{V}{\tau}. \quad (\text{A11})$$

These equations express the behavior of the X and Y components of the low-frequency signal envelope and of U and V , the transverse components of the pseudospins equivalent to the Lorentzian oscillators, in a reference frame traveling at velocity c_0 and rotating with angular velocity $\omega_0 + \partial \phi / \partial t'$.

This set of equations, together with the initial-value conditions, can be solved readily by Laplace transformation. The general solution for the envelope is of the form:

$$A(t', x) = \mathcal{L}^{-1} \{ A(s, x=0) \exp[-\Lambda' x / (s + i \Delta \omega + 1/\tau)] \}, \quad (\text{A12})$$

with $\Lambda'' = \omega_0^2 \gamma_0 \gamma_m / 4c_0^5$. Equation (A12) is identical to Eq. (39) to the extent that Λ'' is equal to Λ . Such is the case when the coupling is not large. Thus we conclude that the slowly varying envelope approximation leads to the approximate dispersion relation described by Eq. (1). This result holds if the inequalities (A3) are satisfied and if the coupling is moderate or small. No restriction is imposed directly on the mode lifetime τ . However, if the phase velocity becomes too different from c_0 , then $\partial\phi/\partial x$ will not remain small compared to ω_0/c_0 and the slowly

varying envelope approximation will eventually fail. Thus, the validity of Eq. (1) extends beyond the Lorentzian approximation, but this extension is ill delimited as it stems from the neglect of small terms in differential equations. It will remain valid as long as the left-hand sides of Eqs. (A4) and (A5) represent the bulk of the propagation phenomenon, i.e., are not too small. The envelope must not vary rapidly but must still vary somewhat if there is a sizable amplitude E or D of the pair-vibration mode, a condition which may be expressed by Eq. (42).

- ¹L. Brillouin, *Wave Propagation and Group Velocity* (Academic, New York, 1960).
- ²G. B. Whitham, *Linear and Non-linear Waves* (Wiley, New York, 1974).
- ³J. A. Stratton, *Electromagnetic Theory* (McGraw-Hill, New York, 1939), p. 331.
- ⁴M. Born and E. Wolf, *Principles of Optics* (Pergamon, Oxford, 1965).
- ⁵A. Sommerfeld, *Optics* (Academic, New York, 1954).
- ⁶O. Avenel, M. Rouff, E. Varoquaux, and G. A. Williams, *Phys. Rev. Lett.* **50**, 1591 (1983).
- ⁷O. Avenel, E. Varoquaux, and G. A. Williams, in *Proceedings of the 17th International Conference on Low Temperature Physics*, edited by U. Eckern, A. Schmid, W. Weber, and H. Wühl (North-Holland, Amsterdam, 1984), p. 767.
- ⁸C. Eckart, *Rev. Mod. Phys.* **20**, 399 (1948).
- ⁹L. A. Wainshtein, *Usp. Fiz. Nauk.* **118**, 339 (1976) [*Sov. Phys.—Usp.* **19**, 189 (1976)].
- ¹⁰A. Sommerfeld, as quoted by Brillouin in Ref. 1, *Phys. Z.* **8**, 841 (1907); *Ann. Phys. (Leipzig)* **44**, 177 (1914).
- ¹¹L. Brillouin, *Ann. Phys. (Leipzig)* **44**, 203 (1914).
- ¹²H. G. Baerwald, *Ann. Phys. (Leipzig)* **7**, 731 (1930).
- ¹³L. A. Wainshtein, *Zh. Tekh. Fiz.* **27**, 2606 (1957) [*Sov. Phys.—Tech. Phys.* **2**, 2420 (1958)]. However, see Ref. 9 for this author's later views.
- ¹⁴J. L. Birman and M. J. Frankel, *Opt. Commun.* **13**, 303 (1975).
- ¹⁵M. J. Frankel and J. L. Birman, *Phys. Rev. A* **15**, 2000 (1977). This paper contains, in particular, an account in modern terms of Baerwald's work.
- ¹⁶A. Puri and J. L. Birman, *Phys. Rev. Lett.* **47**, 173 (1981).
- ¹⁷G. C. Sherman and K. E. Oughstun, *Phys. Rev. Lett.* **47**, 1451 (1981).
- ¹⁸N. S. Shiren, *Phys. Rev.* **128**, 2103 (1962).
- ¹⁹N. S. Shiren, *Phys. Rev. Lett.* **15**, 341 (1965); **15**, 397(E) (1965).
- ²⁰C. G. B. Garrett and D. E. McCumber, *Phys. Rev. A* **1**, 305 (1970).
- ²¹M. D. Crisp, *Phys. Rev. A* **4**, 2104 (1971).
- ²²A. Puri and J. L. Birman, *Phys. Rev. A* **27**, 1044 (1983).
- ²³B. Macke, *Opt. Commun.* **49**, 307 (1984).
- ²⁴F. R. Faxvog, C. N. Y. Chow, T. Bieber, and J. A. Carruthers, *Appl. Phys. Lett.* **17**, 192 (1970).
- ²⁵S. Chu and S. Wong, *Phys. Rev. Lett.* **48**, 738 (1982).
- ²⁶B. Segard and B. Macke, *Phys. Lett.* **109A**, 213 (1985).
- ²⁷O. Avenel, E. Varoquaux, and H. Ebisawa, *Phys. Rev. Lett.* **45**, 1952 (1980), in the inset of Fig. 1.
- ²⁸L. Brillouin, *Congrès International d'Electricité* (Gauthier-Villars, Paris, 1933), Vol. 2, p. 739.
- ²⁹T. A. Weber and D. B. Trizna, *Phys. Rev.* **144**, 277 (1966).
- ³⁰D. L. Johnson, *Phys. Rev. Lett.* **41**, 417 (1978).
- ³¹See *Optics*, Ref. 5, p. 118. Seismic precursors consist of those early microseisms which precede major quakes [O. Jaoul (private communication)].
- ³²P. Pleshko and I. Palócz, *Phys. Rev. Lett.* **22**, 1201 (1969).
- ³³S. L. McCall and E. L. Hahn, *Phys. Rev.* **183**, 457 (1969).
- ³⁴G. L. Lamb, *Rev. Mod. Phys.* **43**, 99 (1971).
- ³⁵M. D. Crisp, *Phys. Rev. A* **1**, 1604 (1970).
- ³⁶M. D. Crisp, *Phys. Rev. A* **5**, 1365 (1972).
- ³⁷F. A. Hopf, G. L. Lamb, C. K. Rhodes, and M. O. Scully, *Phys. Rev. A* **3**, 758 (1971).
- ³⁸H. P. Grieneisen, J. Goldhar, N. A. Kurnit, A. Javan, and H. R. Schlossberg, *Appl. Phys. Lett.* **21**, 559 (1972).
- ³⁹S. M. Hamadani, J. Goldhar, N. A. Kurnit, and A. Javan, *Appl. Phys. Lett.* **25**, 160 (1974).
- ⁴⁰E. Yablonovitch and J. Goldhar, *Appl. Phys. Lett.* **25**, 580 (1974).
- ⁴¹H. S. Kwok and E. Yablonovitch, *Appl. Phys. Lett.* **30**, 158 (1977).
- ⁴²T. Itoh, P. Lavallard, J. Reydellet, and C. Benoit à la Guillaume, *Solid State Commun.* **37**, 925 (1981).
- ⁴³B. Segard and B. Macke, *Opt. Commun.* **38**, 96 (1981).
- ⁴⁴H. J. Hartmann and A. Laubereau, *Opt. Commun.* **47**, 117 (1983).
- ⁴⁵J. E. Rothenberg, D. Grischkowsky, and A. C. Balant, *Phys. Rev. Lett.* **53**, 552 (1984).
- ⁴⁶O. Avenel, E. Varoquaux, and G. A. Williams, *Phys. Rev. Lett.* **53**, 2058 (1984).
- ⁴⁷A. J. Leggett, *Rev. Mod. Phys.* **47**, 331 (1975).
- ⁴⁸P. W. Anderson and W. F. Brinkman, in *The Helium Liquids*, edited by J. G. M. Armitage and I. E. Farquhar (Academic, London, 1975), Chap. 8.
- ⁴⁹D. M. Lee and R. C. Richardson, in *The Physics of Liquid and Solid Helium*, edited by K. H. Bennemann and J. B. Ketterson (Wiley, New York, 1978), Pt. II, Chap. 4.
- ⁵⁰P. Wölfle, in *Progress in Low Temperature Physics*, edited by D. F. Brewer (North-Holland, Amsterdam, 1978), Vol. VIIa, Chap. 3.
- ⁵¹W. P. Halperin, *Physica* **109&110B+C**, 1596 (1982).
- ⁵²J. A. Sauls and J. W. Serene, *Phys. Rev. B* **23**, 4798 (1981).
- ⁵³N. Schopohl and L. Tewordt, *J. Low Temp. Phys.* **45**, 67 (1981).
- ⁵⁴R. Combescot, *J. Low Temp. Phys.* **49**, 295 (1982).
- ⁵⁵P. Wölfle, *J. Phys. (Paris) Colloq.* **6**, C6-1278 (1978).
- ⁵⁶V. E. Koch and P. Wölfle, *Phys. Rev. Lett.* **46**, 486 (1981).
- ⁵⁷O. Avenel, L. Piché, W. M. Saslow, E. Varoquaux, and R.

- Combescot, *Phys. Rev. Lett.* **47**, 803 (1981).
- ⁵⁸L. D. Landau and E. M. Lifshitz, *Quantum Mechanics* (Pergamon, London, 1958), p. 263.
- ⁵⁹H. A. Lorentz, *The Theory of Electrons* (Treubner, Leipzig, 1909/Dover, New York, 1952), p. 154.
- ⁶⁰When $c_m/c_0 \rightarrow 0$, these expressions reduce to the case treated by Lorentz where no spatial dispersion is present. The discussion here follows that given in Ref. 57. We have considered the case where the internal mode displays no spatial dispersion ($c_m=0$) in Ref. 6. The two cases yield very similar results in the framework of the Lorentzian approximation, apart from the existence of a "slow" propagating mode. A detailed discussion of the difference between these two cases is given by Frankel and Birman (Ref. 15).
- ⁶¹This condition is equivalent to Eq. (16) only when $\Gamma < 1 - \sqrt{3}/12$. When $\Gamma \rightarrow 1$ the expansion leading to Eq. (2) or (27) is still valid. We know of no physical system to which the limit $\Gamma \rightarrow 1$ applies.
- ⁶²N. Bogoliubov and I. Mitropolski, *Les Méthodes Asymptotiques en Théorie des Oscillations Non-linéaires* (Gauthier-Villars, Paris, 1962).
- ⁶³The prescriptions of the envelope approximation are not unique and variants leading to results differing from Eq. (41) can be found.
- ⁶⁴S. Chu and S. Wong, *Phys. Rev. Lett.* **49**, 1293 (1982).
- ⁶⁵M. Abramowitz and I. A. Stegun, *Handbook of Mathematical Functions* (Dover, New York, 1965), p. 1026.
- ⁶⁶G. N. Watson, *Treatise on the Theory of Bessel Functions* (Cambridge University Press, Cambridge, 1922).
- ⁶⁷R. Loudon, *J. Phys. A* **3**, 233 (1970).
- ⁶⁸L. Brillouin, *Ann. Ecole Normale (Paris)* **33**, 17 (1916).
- ⁶⁹E. T. Copson, *Asymptotic Expansions* (Cambridge University Press, Cambridge, 1965).
- ⁷⁰A. Erdélyi, *Asymptotic Expansions* (Dover, New York, 1956).
- ⁷¹M. Born and E. Wolf, *Principles of Optics*, Ref. 4, Appendix III.
- ⁷²R. P. Feynman, F. L. Vernon, and R. W. Hellwarth, *J. Appl. Phys.* **28**, 49 (1957).
- ⁷³A. Abragam, *The Principles of Nuclear Magnetism* (Oxford University Press, Oxford, 1962).
- ⁷⁴D. B. Mast, Bimal K. Sarma, J. R. Owers-Bradley, I. D. Calder, J. B. Ketterson, and W. P. Halperin, *Phys. Rev. Lett.* **45**, 266 (1980).
- ⁷⁵I. D. Calder, D. B. Mast, Bimal K. Sarma, J. R. Owers-Bradley, J. B. Ketterson, and W. P. Halperin, *Phys. Rev. Lett.* **45**, 1866 (1980).
- ⁷⁶E. Varoquaux, *J. Phys. (Paris) Colloq.* **6**, C6-1605 (1978).
- ⁷⁷K. Andres and O. V. Lounasmaa, in *Progress in Low Temperature Physics*, edited by D. F. Brewer (North-Holland, Amsterdam, 1982), Vol. VIII, Chap. 4.
- ⁷⁸O. Avenel, P. Berglund, D. Bloyet, P. Roubeau, and E. Varoquaux (unpublished); M. W. Meisel, O. Avenel, and E. Varoquaux (unpublished).
- ⁷⁹B. S. Shivaram, M. W. Meisel, Bimal K. Sarma, W. P. Halperin, and J. B. Ketterson, *J. Low Temp. Phys.* **63**, 57 (1986).
- ⁸⁰B. Mühlischlegel, *Z. Phys.* **115**, 313 (1959).
- ⁸¹A. Savitzky and M. J. E. Golay, *Anal. Chem.* **36**, 1627 (1964).
- ⁸² $Z_Q = 1.52 \times 10^6$ g/s cm² for an X-cut quartz crystal.
- ⁸³E. Polturak, P. G. N. de Vegvar, E. K. Zeise, and D. M. Lee, *Phys. Rev. Lett.* **46**, 1588 (1981).
- ⁸⁴J. A. Sauls, *Phys. Rev. Lett.* **47**, 530 (1981); M. Rouff and E. Varoquaux, *ibid.* **51**, 1107 (1983).
- ⁸⁵R. G. Ulbrich and G. W. Fehrenbach, *Phys. Rev. Lett.* **43**, 963 (1979).
- ⁸⁶The term "0 π " pulse is, in the linear case, a misnomer and should really be reserved for strongly nonlinear features such as those studied by, e.g., E. Y. C. Lu and L. E. Wood, *Appl. Phys. Lett.* **24**, 382 (1974).
- ⁸⁷B. Macke (private communication); B. Macke, J. L. Queva, F. Rohart, and B. Segard (unpublished).
- ⁸⁸O. Avenel, L. Piché, M. Rouff, E. Varoquaux, R. Combescot, and K. Maki, *Phys. Rev. Lett.* **54**, 1408 (1985).
- ⁸⁹E. Courtens and A. Szöke, *Phys. Lett.* **28A**, 296 (1968).